

Observing the quantum behavior of light in an undergraduate laboratory

J. J. Thorn, M. S. Neel, V. W. Donato, G. S. Bergreen, R. E. Davies, and M. Beck^{a)}

Department of Physics, Whitman College, Walla Walla, Washington 99362

(Received 4 December 2003; accepted 15 March 2004)

While the classical, wavelike behavior of light (interference and diffraction) has been easily observed in undergraduate laboratories for many years, explicit observation of the quantum nature of light (i.e., photons) is much more difficult. For example, while well-known phenomena such as the photoelectric effect and Compton scattering strongly suggest the existence of photons, they are not definitive proof of their existence. Here we present an experiment, suitable for an undergraduate laboratory, that unequivocally demonstrates the quantum nature of light. Spontaneously downconverted light is incident on a beamsplitter and the outputs are monitored with single-photon counting detectors. We observe a near absence of coincidence counts between the two detectors—a result inconsistent with a classical wave model of light, but consistent with a quantum description in which individual photons are incident on the beamsplitter. More explicitly, we measured the degree of second-order coherence between the outputs to be $g^{(2)}(0) = 0.0177 \pm 0.0026$, which violates the classical inequality $g^{(2)}(0) \geq 1$ by 377 standard deviations. © 2004 American Association of Physics Teachers.

[DOI: 10.1119/1.1737397]

I. INTRODUCTION

Students often believe that the photoelectric effect, and Einstein's explanation of it, proves that light is made of photons. This is simply not true; while the photoelectric effect strongly suggests the existence of photons, it does not demand it.^{1,2} It was shown in the 1960s by Lamb and Scully that the photoelectric effect can be explained by assuming that the detector atoms are quantized, but that the field is not (i.e., by assuming light to be a classical wave). This explanation is based on the semiclassical model of photoelectric detection, which we will discuss further below.^{3,4}

How then does one prove that photons exist? Here, we will assume that proving photons exist is equivalent to observing an effect that requires a quantum mechanical description of the field; equivalently, we will say that photons exist if the results of an experiment cannot be explained using a classical wave theory of light. Ideally, an experiment to prove the existence of photons will also demonstrate that light has “granular” properties. While physicists may argue about which specific experiment was the first to conclusively demonstrate the existence of a field requiring a quantum mechanical (QM) description, one can be fairly certain that this experiment was carried out in the 1970s.^{5–7} While many such experiments have subsequently been performed, we know of very few that are well-suited for an undergraduate laboratory.^{8–10}

In 1986, Grangier, Roger, and Aspect performed an elegant experiment.^{11,12} Conceptually very simple, their approach was to examine correlations between photodetections at the transmission and reflection outputs of a 50/50 beamsplitter. To quote the experimenters, “a single photon can only be detected once!”¹¹ Hence, if a single quantum of light is incident on the beamsplitter (BS), it should be detected at the transmission output or at the reflection output, but not both: there should be no coincident detections between the two outputs. In fact, Grangier *et al.* measured fewer coincidences than predicted by a classical wave theory, violating a classical inequality by 13 standard deviations, and demonstrating that the field incident on the beamsplitter was well

described by a single-photon state.¹¹ As discussed below in more detail, the key challenge in such a measurement is to create a field that truly has a *single-photon* incident on the BS; a weak beam containing on *average* a single photon (or less) is not sufficient.

Here, we have repeated the experiment of Grangier *et al.*, adapting it for an undergraduate laboratory. We have taken advantage of over 15 years of technological advancements to obtain orders of magnitude increased count rates over those obtained by Grangier *et al.* The increased count rate in our experiment allows us to violate a classical inequality by 146 standard deviations with only 5 min of counting time. Our experiment is well described by the QM description of a field in a single photon state incident on a beamsplitter.

II. HISTORY AND THEORY

A. Early measurements

As stated above, we are interested in examining correlations between the photocounts on two detectors situated at the output ports of a BS (Fig. 1). The first experiment to examine these correlations was carried out by Hanbury Brown and Twiss,^{13,14} who found a positive correlation between the outputs of the two detectors. It should be noted that in this first experiment, Hanbury Brown and Twiss were not counting individual photons, but were instead measuring correlations between continuous currents from photomultiplier tubes (PMTs).¹³ As such, this positive correlation indicated that when the current from one PMT increased, the current on the second tended to increase simultaneously. While the intent of Hanbury Brown and Twiss was to develop a new technique for measuring the angular diameter of stars,¹⁵ their work played an important role in creating the field of quantum optics.

A brief controversy arose when Brannen and Ferguson performed a similar experiment in which they observed no positive correlation, and then claimed “that if such a positive correlation did exist, it would call for a major revision of some fundamental concepts in quantum mechanics.”¹⁶ However, Purcell¹⁷ and Hanbury Brown and Twiss¹⁸ quickly

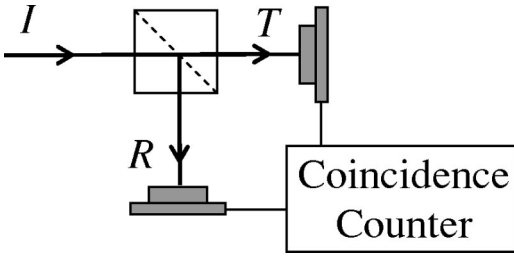


Fig. 1. Coincidence measurement. The incident (I) beam is split into transmitted (T) and reflected (R) beams at a 50/50 BS. Detections at T and R are examined to see whether or not they occur simultaneously.

noted that the experimental parameters used by Brannen and Ferguson precluded the observation of positive correlations. They also showed that positive correlations are not only allowed by quantum mechanics, but are a natural consequence of the tendency for photons (and other bosons) to “bunch” together. The first experiment to observe positive correlations using coincidence detection of individual photocounts (not just photocurrents) from PMTs was performed by Twiss, Little, and Hanbury Brown,¹⁹ who observed positive correlations of a few percent. This amount of correlation was consistent with that expected, given their experimental parameters.

B. Classical fields

By a classical field, we mean an electromagnetic wave that is perfectly described by Maxwell’s equations. For such a field, the correlations between the intensities of the transmitted I_T and reflected I_R beams are given by the *degree of second-order (temporal) coherence*, $g_{T,R}^{(2)}(\tau)$, which is a function of the time delay τ between the intensity measurements:²⁰

$$g_{T,R}^{(2)}(\tau) = \frac{\langle I_T(t+\tau)I_R(t) \rangle}{\langle I_T(t+\tau) \rangle \langle I_R(t) \rangle}. \quad (1)$$

If the light source is *stationary* (i.e., if its statistics do not change in time), then we can interpret the brackets as referring to ensemble averages rather than time averages. It is called the degree of second-order coherence because it involves correlations between intensities, whereas the degree of first-order coherence describes correlations between fields.

Of particular importance to the present work is the case of simultaneous ($\tau=0$) intensity measurements. In this case, and furthermore assuming a 50/50 BS in which the transmitted, reflected, and incident intensities are related by $I_T(t) = I_R(t) = \frac{1}{2}I_I(t)$, it is straightforward to see that

$$g_{T,R}^{(2)}(0) = g_{I,I}^{(2)}(0) = \frac{\langle [I_I(t)]^2 \rangle}{\langle I_I(t) \rangle^2} = g^{(2)}(0). \quad (2)$$

From the Cauchy–Schwartz inequality, it is straightforward to prove that $\langle I_I(t) \rangle^2 \leq \langle [I_I(t)]^2 \rangle$.^{20,21} Using this, we find that

$$g_{T,R}^{(2)}(0) = g^{(2)}(0) \geq 1 \quad (\text{classical fields}), \quad (3)$$

where we emphasize that this result has been derived using classical wave theory. In Eq. (3), equality with 1 is achieved if the input field is perfectly stable with no fluctuations, while for fluctuating fields the second-order coherence is greater than 1. For “chaotic” light (e.g., light from a thermal

source that is either collisionally or Doppler broadened), it can be shown that $g^{(2)}(0) = 2$.²⁰ In an ingenious set of experiments involving a “pseudothermal” light source (a laser whose phase was randomized by a rotating ground-glass slide), Arrechi *et al.* were able to measure fields with $g^{(2)}(0) = 1$ and $g^{(2)}(0) = 2$.²²

C. Semiclassical theory of photodetection

So far, we have been speaking about correlations between the intensities of the fields leaving the BS. In an experiment, however, one does not measure the intensity directly, but rather the photocurrent from a detector. It is then necessary to model the photodetection process. Since to this point we have been discussing classical fields, it is most appropriate to use a model that treats the field classically. The most rigorous theory of this sort is the semiclassical theory of photoelectric detection, in which the field is treated classically and the photodetector is treated quantum mechanically.²³ For the purposes of the discussion here, it is convenient to refer to the detector monitoring the transmitted (reflected) field as detector T (R).

In the semiclassical theory of photoelectric detection, it is found that the conversion of continuous electromagnetic radiation into discrete photoelectrons is a random process. The probability of obtaining a single photocount from a single detector (for example, detector T) within a short time window Δt is proportional to the average intensity of the field striking that detector, given as

$$P_T \Delta t = \eta_T \langle I_T(t) \rangle \Delta t, \quad (4)$$

where η_T is a constant that characterizes the detection efficiency of detector T . The joint probability of obtaining a photocount (within a time window Δt) at detector R , and then after a time τ obtaining a photocount at detector T (within a time window Δt), is given by

$$P_{TR}(\tau) \Delta t^2 = \eta_T \eta_R \langle I_T(t+\tau)I_R(t) \rangle \Delta t^2. \quad (5)$$

It is then easily seen that if one measures the probability of joint and individual photocounts at detectors T and R , one can determine the degree of second-order coherence from

$$g_{T,R}^{(2)}(\tau) = \frac{P_{TR}(\tau)}{P_T P_R}. \quad (6)$$

Again, we are most interested in simultaneous, $\tau=0$, detection of photocounts at detectors T and R , which occurs with probability $P_{TR}(0)$. Using Eq. (3), we find that for classical fields, the measured degree of second-order coherence must be greater than or equal to 1:

$$g_{T,R}^{(2)}(0) = \frac{P_{TR}(0)}{P_T P_R} = g^{(2)}(0) \geq 1 \quad (\text{classical fields}). \quad (7)$$

Here, we see that if the joint probability factorizes, $P_{TR}(0) = P_T P_R$, which occurs when the detections at T and R are completely uncorrelated, then $g^{(2)}(0)$ is minimized and is equal to 1.

We can summarize what we have learned about classical field statistics as follows. It is possible to measure the degree of second-order coherence between the fields leaving a beamsplitter $g^{(2)}(0)$ by measuring the probability of joint and individual photocounts at detectors T and R . The second-order coherence must satisfy the inequality $g^{(2)}(0) \geq 1$.

When the photocounts at T and R are completely uncorrelated, $g^{(2)}(0)=1$, which occurs when the input field to the beamsplitter is a perfectly stable wave. If the input field fluctuates, then $g^{(2)}(0)>1$, indicating positive correlations between the photocounts.

Since $g^{(2)}(0)$ cannot be less than 1, we are left with the conclusion that for classical fields the measured photocounts at T and R cannot be anticorrelated. This makes sense because a BS simply splits a classical input field into two identical copies. These output fields either fluctuate together (positive correlation) or do not fluctuate at all (no correlation). It is not possible for the intensity of one to decrease while the intensity of the other increases (anticorrelation).

D. Quantum fields

From the time of the original Hanbury Brown and Twiss experiment in 1956,¹³ the importance of a rigorous theory of photoelectric counting was recognized. The first attempts were the semiclassical theories discussed in the previous section. In the mid-1960s sophisticated fully QM theories, in which both the electromagnetic field and the detector atoms are treated quantum mechanically, were developed by Kelly and Kleiner,²⁴ Glauber,²⁵ and others (see Refs. 20 and 23, and the references therein). A QM field is not fully described by Maxwell's equations.

In the fully quantum theory, the correlations between the output fields from the BS in Fig. 1 are still described by the degree of second-order coherence $g_{T,R}^{(2)}(\tau)$, although now the electric fields (and corresponding intensities) are treated as QM operators, rather than as classical waves. Again, we are interested in simultaneous ($\tau=0$) detection of photons at the outputs; quantum mechanically $g_{T,R}^{(2)}(0)$ is defined as

$$g_{T,R}^{(2)}(0) = \frac{\langle : \hat{I}_T \hat{I}_R : \rangle}{\langle \hat{I}_T \rangle \langle \hat{I}_R \rangle}. \quad (8)$$

Here the colons indicate that the creation \hat{a}^\dagger and annihilation \hat{a} operators corresponding to the electric fields are to be placed in normal order, which means that all creation operators appear to the left of all annihilation operators. The intensity operator is proportional to the photon number operator for the field $\hat{n} = \hat{a}^\dagger \hat{a}$, so that

$$g_{T,R}^{(2)}(0) = \frac{\langle : \hat{n}_T \hat{n}_R : \rangle}{\langle \hat{n}_T \rangle \langle \hat{n}_R \rangle} = \frac{\langle \hat{a}_T^\dagger \hat{a}_R^\dagger \hat{a}_R \hat{a}_T \rangle}{\langle \hat{a}_T^\dagger \hat{a}_T \rangle \langle \hat{a}_R^\dagger \hat{a}_R \rangle}, \quad (9)$$

where we have explicitly placed the field operators in normal order.

The averages in Eqs. (8) and (9) are given by QM expectation values. The expectation value is computed using the field states at the detectors. These states can be derived from the input state to the BS.^{23,26} Alternatively, the operators for the reflected and transmitted fields can be written in terms of the operators for the input field \hat{a}_I , and the unoccupied (vacuum) field \hat{a}_V that enters the unused port of the BS (Fig. 2). For a 50/50 BS, and one particular choice of phase for the BS, it is straightforward to show that

$$\hat{a}_R = \frac{1}{\sqrt{2}}(\hat{a}_I + \hat{a}_V), \quad \hat{a}_T = \frac{1}{\sqrt{2}}(\hat{a}_I - \hat{a}_V). \quad (10)$$

Substituting the reciprocity relations Eq. (10) into Eq. (9), and using the fact that the unoccupied field mode is in a

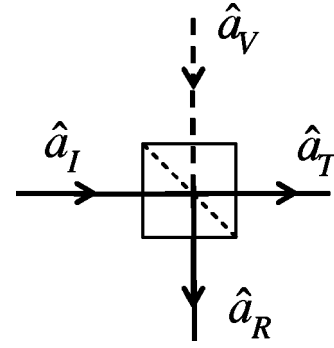


Fig. 2. Field operators corresponding to BS input and output ports.

vacuum state, the second-order coherence can be rewritten as²⁰

$$g_{T,R}^{(2)}(0) = \frac{\langle \hat{n}_I(\hat{n}_I - 1) \rangle}{\langle \hat{n}_I \rangle^2} = g_{I,I}^{(2)}(0) = g^{(2)}(0), \quad (11)$$

where now the expectation value is computed using the QM state of the field incident on the BS. As in the classical case, the second-order coherence between the BS outputs is equal to the second-order coherence of the input.

Quantum mechanically, the measured correlations at the detectors are determined by the state of the field incident on the BS (the input state). The QM equivalent to a stable classical wave is a coherent state $|\alpha\rangle$, which is the eigenstate of the annihilation operator $\hat{a}|\alpha\rangle = \alpha|\alpha\rangle$.²⁰ If one evaluates the second-order coherence [Eq. (11)], assuming an input field in a coherent state, one finds $g^{(2)}(0)=1$, which is the same as the classical result for a stable classical wave. Evaluating Eq. (11) assuming an input field in a thermal state (which is an incoherent mixture described by a density operator) one finds $g^{(2)}(0)=2$.²⁰ Such a field is said to be “bunched,” because one interpretation of this result is that the photons tend to come in bunches; once they strike the BS, some are transmitted and others are reflected, leading to positive correlations between the output fields.

Thus, the quantum theory of photoelectric detection is in agreement with the classical theory described in Sec. II, as long as one uses the appropriate field states. However, there exist certain field states that are inherently QM in nature, and for which there is no classical wave theory counterpart. Such nonclassical fields are not in general constrained by the limits discussed in Sec. II C. An example of a nonclassical field state is one containing exactly one photon; this state is an eigenstate of the photon number operator, with eigenvalue 1: $\hat{n}|1\rangle = 1|1\rangle$. Evaluating Eq. (11) using an input field in a single-photon state yields $g^{(2)}(0)=0$, which violates the classical inequality $g^{(2)}(0) \geq 1$.

Theoretically predicting the existence of nonclassical fields, and generating them in the laboratory, however, are two very different matters. One of the first experiments to demonstrate the existence of a nonclassical field was performed by Kimble, Dagenais, and Mandel in 1977.⁷ They measured the light emitted by a single atom (“resonance

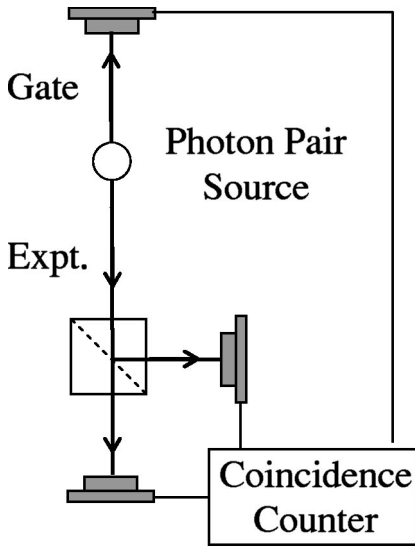


Fig. 3. Coincidence measurements with a gate. A source emits pairs of photons simultaneously, and the photons travel in opposite directions. Detection of the gate signal tells the T and R detectors when to expect a “proper” detection on the experiment side.

fluorescence”) and found $g^{(2)}(0) = 0.4 \leq 1$, proving that the field was “anti-bunched.” An anti-bunched field can be interpreted as one in which the photons do not clump together, and hence tend to arrive one at a time. When these individual photons strike the beamsplitter, they are either transmitted or reflected (but not both), leading to anticorrelations in the photocounts at the detectors.

Despite clearly demonstrating that the light emitted by a single atom is anti-bunched, this experiment was complicated by the difficulty of isolating the light coming from the atom from the background scattered light. This complication was due to the fact that the laser light used to excite the atom and the resonance fluorescence were both at the same frequency. To isolate the resonance fluorescence, it was necessary to use a detailed model of the experiment, and to correct for the expected contribution from the scattered laser light.

A conceptually much simpler demonstration of photon anti-bunching was performed by Grangier, Roger, and Aspect in 1986.¹¹ A schematic of their experiment is shown in Fig. 3. They circumvented the problem of background light by using a two-photon cascade in Ca. In this process, a Ca atom absorbs two photons, one each from two lasers operating at frequencies ν_{11} and ν_{12} , promoting it to an excited state. The Ca atom then decays by emitting two photons at different frequencies: one at frequency ν_1 by decaying to a short-lived intermediate level, and a second at frequency ν_2 by decaying to the ground state. All four frequencies are distinct and can be isolated using filters, greatly reducing the problem of scattered background from the intense laser beams. Furthermore, angular momentum conservation ensured that the two photons always were emitted in opposite directions. The detection of one photon at one detector ensured that there would be a photon heading in the opposite direction, so that the first photon could be used as a gate to tag the arrival of the second. Thus, when a gate photon was detected, it was known with high confidence that there was one (and only one) photon incident on the BS.

For this experiment, detections at T and R were condi-

tioned upon detections at the gate detector (detector G). With this conditioning, the measured degree of second-order coherence [Eq. (6)] is given by

$$g^{(2)}(0) = \frac{P_{GTR}}{P_{GT}P_{GR}}. \quad (12)$$

Here, $P_{GT}(P_{GR})$ is the probability of measuring simultaneous photocounts at detector $T(R)$ and detector G , and P_{GTR} is the probability of obtaining a threefold coincidence between detectors T , R , and G . The probabilities can be written as

$$P_{GTR} = \frac{N_{GTR}}{N_G}, \quad P_{GT} = \frac{N_{GT}}{N_G}, \quad P_{GR} = \frac{N_{GR}}{N_G}, \quad (13)$$

where, given a specified time window, $N_{GT}(N_{GR})$ is the number of simultaneous photocounts at detector $T(R)$ and detector G , N_{GTR} is the number of threefold coincidences, and N_G is the number of singles counts at detector G . By using Eq. (13), we can rewrite the experimentally determined degree of second-order coherence [Eq. (12)], as

$$g^{(2)}(0) = \frac{N_{GTR}N_G}{N_{GT}N_{GR}}. \quad (14)$$

In an experimental tour-de-force, Grangier *et al.* measured a second-order coherence of $g^{(2)}(0) = 0.18 \pm 0.06$, which violated the classical inequality $g^{(2)}(0) \geq 1$ by 13 standard deviations.¹¹ In a 5 h experiment, they measured a total of nine threefold coincidences, while a classical wave theory would have predicted greater than 50 threefold coincidences. If the state were a perfect one-photon state, Grangier *et al.* would have measured no threefold coincidences.

We have repeated the experiment of Grangier *et al.*; with advances in technology over the past 15+ years, however, a tour-de-force is no longer required. By using only readily available, off-the-shelf components, we were able to assemble this experiment in an undergraduate laboratory. In a typical run lasting less than 5 min, we measure $g^{(2)}(0) = 0.0188 \pm 0.0067$, where no corrections have been applied to the data to account for accidental coincidences. We have also determined that by accounting for the expected accidental coincidences (see Appendix A), the difference between our result and $g^{(2)}(0) = 0$ (i.e., that expected from a true single-photon incident on the BS) is fully explained by the accidental coincidences.

III. PARAMETRIC DOWNCONVERSION

The key to our ability to perform the experiment is our use of a parametric down-conversion source in place of the atomic Ca cascade source used by Grangier *et al.*¹¹ This method has the advantages of increased simplicity, reduced cost, and increased count rates (several orders of magnitude greater than those observed by Grangier *et al.*) In the process of spontaneous parametric downconversion, a single photon of one frequency is converted into two photons of lower frequency (by approximately a factor of 2). Although downconversion is extremely inefficient (milliwatts of input power generate output beams that must be detected using photon counting), it is much more efficient than the Ca cascade.

The input is referred to as the pump (at angular frequency ω_p), while the two outputs are referred to as the signal and idler (at angular frequencies ω_s and ω_i). Energy conservation requires that

$$\hbar \omega_p = \hbar \omega_s + \hbar \omega_i, \quad \omega_p = \omega_s + \omega_i. \quad (15)$$

Momentum conservation is equivalent to the classical phase-matching condition, which requires that the wave vectors of the input and output fields satisfy

$$\vec{k}_p = \vec{k}_s + \vec{k}_i. \quad (16)$$

The frequencies and wave vectors are not independent of each other, and are related by the dispersion relation

$$k_p = \frac{n_p(\omega_p) \omega_p}{c}, \quad (17)$$

where $n_p(\omega_p)$ is the index of refraction of the pump wave at the pump frequency, and similarly for the signal and idler waves.

In Type-I downconversion, which is what we use in our experiments, the signal and idler beams are polarized parallel to each other, and their polarization is perpendicular to that of the pump; all polarizations are linear. By proper orientation of the pump beam wave vector \vec{k}_p with respect to the optic axis of the crystal, it is possible to satisfy the constraints imposed in Eqs. (15)–(17). Because only the relative angle between the pump, signal, and idler are important, the downconverted light is emitted into a cone surrounding the pump beam (see, for example, Ref. 9).

Typically, the frequencies of the signal and idler beam are chosen to be equal to each other, at half the frequency (twice the wavelength) of the pump. In order to separate the signal and idler, they are chosen to make a small angle (a few degrees) with the pump beam so that the signal comes out a few degrees from the pump, and the idler comes out a few degrees on the other side of the pump.

However, for a given crystal orientation, there is no unique solution to the constraints imposed in Eqs. (15)–(17). The sums of the frequencies and wave vectors are constrained, but not the individual frequencies and wave vectors. For instance, if the signal frequency is less than half the pump frequency by a certain amount, it is possible for energy to be conserved [Eq. (15)], if the idler frequency is an equal amount greater than half the pump frequency. In order for momentum to be conserved [Eq. (16)], the signal makes a slightly greater angle with respect to the pump, and the idler makes a slightly smaller angle. Thus, the light coming out of a downconversion crystal is emitted into a range of angles (several degrees), and wavelengths (on the order of 10s of nm, centered about twice the pump wavelength).

The similarity between the Ca cascade source used by Grangier *et al.*¹¹ and our downconversion source is that both sources produce two photons, one of which is used as a gate. In our experiment, we use the idler photons as a gate—the detection of an idler photon in one beam (using detector *G*) indicates that there is a signal photon present in the other. The signal beam is directed to a beamsplitter with two detectors at its outputs (detectors *T* and *R*). Just as in the experiment of Grangier *et al.*, we expect to see an absence of coincidences between the *T* and *R* detectors, conditioned on a detection at *G*. This absence is equivalent to an absence of threefold coincidences between *G*, *T*, and *R*. We can use Eq.

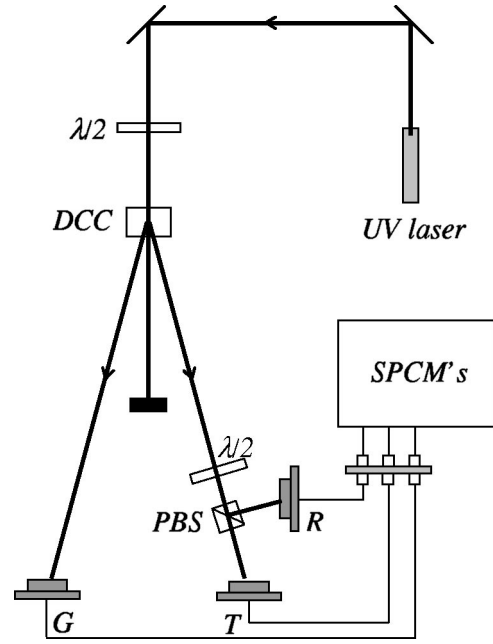


Fig. 4. Experimental apparatus. Major components include an ultraviolet laser, downconversion crystal (DCC), polarizing beamsplitter (PBS), single-photon counting modules (SPCM's), and gating, transmission-side, and reflection-side collection optics (*G*, *T*, *R*). Optical fibers direct the light from *G*, *T*, and *R* to their corresponding SPCMs.

(14) as a measure of the second-order coherence of the signal beam, and a result of $g^{(2)}(0) < 1$ is inconsistent with a classical wave description of our system.

IV. EXPERIMENT

We now describe the major components for our updated version of the experiment of Grangier *et al.* The layout of these components is presented in Fig. 4. In brief, a beam of ultraviolet laser light enters a nonlinear crystal where, via spontaneous parametric downconversion, some of the light is converted into IR light in two beams. Light from one of the IR beams (the idler) is used as a *gating beam* and passes directly from the crystal into a photodetector. Light from the other beam (the signal), which we shall call the *experiment beam*, is directed into a 50/50 BS and subsequently observed by photodetectors placed in both the transmission and reflection ports of the beamsplitter. A photodetection in the gating beam is used to signal that the experiment beam has been prepared in the proper single-photon state, and it is the light in the experiment beam whose second-order coherence is measured. Detections from the three detectors *G*, *T*, and *R* are registered by a series of time-to-amplitude converters and single-channel analyzers; coincidence statistics are then compiled and analyzed.

For a more detailed discussion, it is convenient to group components of the instrument into three categories: (i) light source, (ii) light detection, and (iii) coincidence-counting electronics; there also are some diagnostic instruments that make the experiments easier to perform. A list of major components, manufacturers, and part numbers is provided in Appendix C; all of the equipment is commercially available and relatively affordable; a complete parts list and further information is available on our website.²⁷

A. Light source

Our light source was designed to be sufficiently bright so that alignment can be done in real time; we obtain sufficient coincidences in a 100-ms counting window to use the ~ 10 -Hz rate of raw coincidence measurements to perform final alignment. Given this high brightness, data collection occurs over a few minutes (our experimental runs last from approximately 5 to 40 min).

The pump laser used in this work is a cw ultraviolet (409 nm), diode-pumped, frequency-doubled, solid-state laser; the pump is linearly polarized. It was chosen for its turnkey operation, high output power (20 mW), long advertised lifetime (10 000 h) and comparative value. Before entering the downconversion crystal, the pump passes through a zero-order, 400-nm half-wave plate, which allows us to adjust the pump polarization to maximize the downconversion rate (by rotating a half-wave plate in its mount, the direction of linear polarization also rotates.) Downconversion is accomplished in a 5×5 mm aperture, 3-mm-long beta-barium borate (BBO) crystal. It is cut for Type-I downconversion of 405-nm pump light, with a 810-nm signal and idler waves making angles of $\theta = 3^\circ$ with respect to the pump. Because the crystal is hygroscopic, the crystal faces have humidity-barrier, antireflective coatings. The crystal is mounted so that a small flow of dry nitrogen flows over it while in use on the optical table. When not in use, the crystal is stored in a desiccant jar.

When discussing the performance of the source, it is useful to talk in terms of the count rates R , measured in counts per second (cps); $R_G = N_G / \Delta T$, where ΔT is the measurement time, and similarly for other count rates. Our source regularly produces singles count rates in the signal and idler beams (e.g., R_G) of $\sim 110\,000$ cps, and total coincidence rates between the signal and idler beams of ~ 8800 cps (coincidence rates for the counters behind the BS, R_{GT} and R_{GR} are half this value.)

The downconverted light is vertically polarized. Instead of using an ordinary 50/50 BS, we use a combination of a half-wave plate and a polarizing beamsplitter (PBS). The half-wave plate is adjusted so that the light entering the PBS is polarized at 45° with respect to the polarization axis of the PBS; the light then splits equally between the two outputs. By rotating the half-wave plate, we can adjust the input polarization (and hence the splitting ratio), allowing us to fine tune the splitting to be as close to 50/50 as possible. We also can easily transmit or reflect 100% of the beam, which is useful during alignment.

B. Light detection

Our light collection optics are designed for ease of alignment and ambient light rejection. The use of fiber optic cables also makes the system very flexible. We highly recommend that anyone performing experiments with downconverted light consider using a similar fiber-based system.

The collection optics and detection systems for the three detectors (G , T , and R) are identical. Downconverted light is collected by a converging lens and focused into the end of a $62.5\text{-}\mu\text{m}$ -diameter, 1-m-long multimode fiber optic cable that has fiber-coupling (FC) connectors on both ends. The lens is a fiber-coupling lens (Thorlabs F220FC-B), and is pre-aligned to place the tip of the fiber cable in the focal plane of the lens, so that no alignment of the lens to the fiber is necessary. The other end of the fiber connects to a fiber-to-

fiber coupler, which couples light into a second, identical, fiber. This arrangement allows us the flexibility of swapping connections between the coupling lenses and different detectors, which is useful in setting up the coincidence counting electronics (detailed below). It also allows us to easily connect a fiber-coupled laser diode which shines light backward through the coupling lens onto the downconversion crystal for alignment purposes (detailed below). The second fiber carries the downconverted light into a light-tight enclosure which houses the optical filters and detectors. The only light entering this enclosure comes through the fibers, which greatly eliminates problems with stray light.

Light is coupled out of the second fiber with another fiber-coupling lens, passes through an RG 780 filter (which passes wavelengths longer than 780 nm), and is coupled with a third lens into a third fiber cable ($50\text{-}\mu\text{m}$ diameter, FC connectors, and an opaque jacket). We use a kinematic mount to align the output of one lens with the input of the other. We also surround the lenses and filter with beam tubes to further eliminate the possibility of collecting ambient light. The third fiber cable transports the light to the single-photon counting module (SPCM), which has its own FC connector which is pre-aligned to image the fiber tip onto the active area of the detector.

The SPCMs use an avalanche photodiode operated in Geiger mode to detect the light. They output a 30 ns, 4.5 V (into $50\ \Omega$) pulse when they detect a photon, with a 50 ns dead time between pulses. The SPCMs have a specified quantum efficiency of $\sim 50\%$ at 810 nm, and the model we used had dark count rates of ~ 250 cps. With this dark count rate and our 2.5-ns coincidence window, coincidences due to dark counts are negligible.

C. Coincidence counting electronics

As described above, we are interested in detecting coincidence counts between the outputs of different detectors. We use a coincidence window of 2.5 ns, and coincidences are determined using a combination of a time-to-amplitude converter (TAC) and a single-channel analyzer (SCA). Three such coincidence units are used (one each for GT , GR , and GTR coincidences), and their outputs are recorded by a counting board in our computer. We briefly describe how we use the TAC/SCA to determine twofold GT coincidences. (GR coincidences are determined in the same manner). Modification of the TAC/SCA configuration to obtain threefold GTR coincidences also is described.

A TAC operates by receiving two inputs, called START and STOP, and then outputting a pulse, the amplitude of which is proportional to the time interval between the rising edges of the START and STOP signals. The proportionality between the amplitude and the time interval is controlled by the gain of the TAC, and we typically use a value of 0.2 V/ns. To measure GT coincidences, the START input comes from the output of detector G and the STOP input comes from detector T (see Fig. 5). To ensure that the START pulse precedes the STOP pulse, we insert an extra length of coaxial cable, corresponding to a delay of ~ 6 ns, between T and the STOP input. Thus, if detectors G and T record simultaneous detections, the delay between START and STOP signals is 6 ns, and the output from the TAC is 1.2 V.

The SCA operates by receiving an input pulse, and then outputting a pulse (with an amplitude of 5 V) *only* if the amplitude of the input pulse falls within a certain voltage window. The width of the window is adjustable, as is the

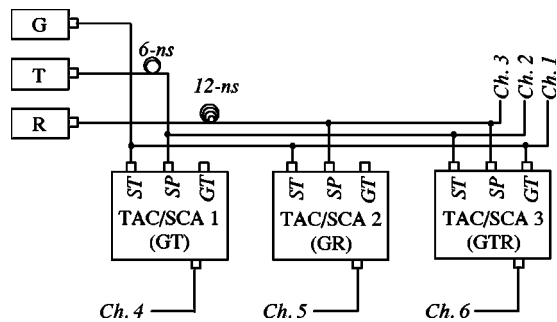


Fig. 5. Coincidence counting electronics. TACs and SCAs are used to identify GT , GR , and GTR coincident detections. Here ST , SP , and GT refer to START, STOP, and START GATE inputs, respectively. The outputs go to six input channels on the counter.

lower level of the window. The input to the SCA is the output from the TAC. Using the values for the TAC output above, a coincidence window of 2.5 ns centered about 6 ns corresponds to a voltage range of 0.95–1.45 V, and our SCA is configured to output a pulse if the amplitude of the input pulse lies within this range. The only trick to configuring the TAC/SCA setup is in properly setting the SCA window to maximize true coincidences and reject false coincidences. This procedure is described in Appendix B.

In order to measure the threefold GTR coincidences, we use T as the START input and R as the STOP input, and configure the TAC/SCA as described above to register TR coincidences. To ensure that these TR coincidences also are coincident with a detection at G , we operate the TAC in “start gate coincidence” mode, and feed the G signal to the START GATE input of the TAC. If an output pulse from G is not present at the START GATE when the pulse from T arrives at START, then the timing circuitry in the TAC is disabled, and no output is produced.

There is one last trick used in setting up this threefold coincidence unit. The technique for setting the SCA window described in Appendix B relies on observing coincidences between the detectors measuring the START and STOP input; however, we expect an *absence* of coincidences between T and R . In order to obtain coincidences between these detectors so that we can set the window, we switch the fiber optic cables so that the idler (gate) beam is fed into the detector that ordinarily measures the R output. Now, we have coincident photons entering the two detectors, so that we can set the window as described in Appendix B. The delays are all set by the coaxial (electrical) cables between the detectors and the coincidence units. Because all of the fiber cables have the same length, the optical delays are the same, and switching the fiber cables back after the window is set does not affect the timing.

We measure a total of six photocounts in each data acquisition interval: singles counts from each of the three detectors, N_G , N_R , and N_T , as well as the coincidence counts N_{GR} , N_{GT} , and N_{GTR} . We use a counting board that plugs into a PCI slot in our computer, and it simultaneously records these counts on six different channels. A LABVIEW program reads the data from the board, computes the second-order coherence [Eq. (14)], and saves the data.

D. Optical alignment

Although requiring some care, we have found the setup and alignment process to be sufficiently straightforward that two undergraduates having some familiarity with the experiment were able to start from a bare optical table and complete the process with minimal supervision over the course of one or two days. The alignment is robust once it has been completed. For example, we remove the downconversion crystal when it is not in use; reinserting the crystal and tweaking-up the alignment takes only a few minutes. When starting from scratch, the major components are first affixed to the optical table in rough alignment as illustrated in Fig. 4; although at first we are interested solely in obtaining coincidences between the idler and signal beams, so that the half-wave plate, PBS, and detector R are not used. The pump beam is aligned level to the table using the two mirrors, and the electrical connections are completed.

The first component to be aligned is the collection optics (i.e., fiber optic cable/lens assembly) for the G detector. The collection lens is mounted in a kinematic mount that allows for horizontal, vertical, and angular adjustment, and the center height of the lens is adjustable using a post holder and post. The height is initially adjusted so that the center of the lens is at the same height as the pump beam. Light from a fiber-coupled 780 nm laser diode is coupled (via the fiber-to-fiber coupler) backward through the fiber cable, and out through the lens. The lens is placed so that angle of this beam is set to be 3° off of the pump beam, and the mount is adjusted so that the laser shines back onto the center of the downconversion crystal. The alignment laser is now removed and the fiber cable is connected to the detector. By monitoring the count rate from the G detector, the polarization of the pump and the horizontal and vertical tilt of the downconversion crystal are adjusted to maximize the count rate. Once this adjustment has been accomplished, the kinematic mount controlling the alignment of the two lenses surrounding the RG780 filter also is adjusted to maximize the count rate. Now, the horizontal placement of the collection lens (and hence the angle between the collection lens and the pump beam) is carefully adjusted to maximize the count rate. The alignment of the downconversion crystal and placement of the collection beam is then iterated to maximize the count rate on the G detector. As stated above, we typically obtain $\sim 100\,000$ cps on this beam.

Next, the T detector is aligned in nearly the same way. At first the goal is not to painstakingly align this detector for maximum counts, but simply to get enough counts so that the coincidence window between the G and T detectors can be set as described in Appendix B. Once this alignment is set, the alignment of the T collection optics is adjusted to maximize the *coincidence* rate between G and T , not the raw count rate on T . We easily obtain a coincidence rate of over 7000 cps, and frequently achieve a rate of ~ 8800 cps. Once the alignment of the T optics has been accomplished, the alignment laser is shone backward through this optics, and adjustable iris diaphragms are aligned with the beam in between the downconversion crystal and the T optics. These irises serve to identify the beam path and assist in aligning the R detector.

The half-wave plate and PBS are now inserted, and the alignment laser is shone backward through the collection optics of the R detector. The optics are adjusted so that the light goes back through the irises and onto the crystal. The R detector is connected and when counts are achieved, the win-

Table I. Measurements of $g^{(2)}(0)$, the degree of second-order coherence.

Trial (Total acquisition time, min)	Integration time per point (s)	Number of points	$g^{(2)}(0)$	Standard deviation of $g^{(2)}(0)$
1 (~5)	2.7	110	0.0188	0.0067
2 (~10)	5.4	108	0.0180	0.0041
3 (~20)	11.7	103	0.0191	0.0035
4 (~40)	23.4	100	0.0177	0.0026

dow on the *GR* coincidence unit is set, and the *GR* coincidence count is maximized. Lastly, the *GTR* coincidence unit is configured using the procedure described above.

V. RESULTS

One of the primary advantages of the apparatus described in this paper is the ability to acquire good counting statistics in time periods reasonable for an undergraduate laboratory. In Table I, we present the results of four experimental runs. In each of these runs, we performed ~ 100 measurements of $g^{(2)}(0)$, while in each run we changed the integration time for each measurement. These results are clearly inconsistent with a classical wave theory, which predicts $g^{(2)}(0) \geq 1$. Even for counting times of less than 5 min, we obtain a value of $g^{(2)}(0)$ that is lower than the classical lower limit by 146 standard deviations. Increasing the counting time does not affect the measured value of $g^{(2)}(0)$ (to within the statistical error of our measurement), but increasing the counting time does decrease the statistical error. Our best results is $g^{(2)}(0) = 0.0177 \pm 0.0026$, which violates the classical inequality by 377 standard deviations.

If a truly single-photon state were incident on the BS, QM would predict that $g^{(2)}(0) = 0$. Why don't we see this? A consequence of defining a "coincidence" with a finite time window is an expected nonzero anticorrelation parameter. This is because there is the possibility that uncorrelated photons from different downconversion events may hit the *T* and *R* detectors within our finite coincidence window; these are "accidental" coincidences. As the count rates and coincidence window increase, so do the number of accidental coincidences. In Appendix A, we analyze the effect of these accidental coincidences on our measurements of $g^{(2)}(0)$. For our experimental parameters, when we account for accidental coincidences, we calculate an expected value of the second-order coherence $g^{(2)}(0) = 0.0164$, which is what we observe to within our statistical error.

As a final check on the instrument and method, the measurement was repeated, but with an extra length of coaxial cable (corresponding to a delay of 6 ns) placed after the *R* detector. In this case we are not measuring true coincidences, but instead coincidences between measurements made at time t at detector *R*, and time $t + 6$ ns for detector *T*. This means we do not measure the quantity $g^{(2)}(\tau = 0)$, but instead we measure $g^{(2)}(\tau = 6 \text{ ns})$. Under such circumstances, *GTR* coincidences are not excluded because we expect the detections at *T* and *R* to be due to uncorrelated downconversion events. Indeed, we would expect to obtain a measured

value $g^{(2)}(\tau = 6 \text{ ns}) \geq 1$. In two different experimental runs we obtained measured values for $g^{(2)}(\tau = 6 \text{ ns})$ in the range 2–3.

VI. CONCLUSIONS

We have performed an experiment whose results cannot be explained using a classical wave description for light. The results are consistent with a quantum mechanical description in which a field in a single-photon state is incident on a beamsplitter, and as such we take this experiment as proof of the existence of photons. The experiment is conceptually simple, and is suitable for an undergraduate laboratory.

While we would not describe the cost of this experiment as inexpensive (total cost of $\sim \$40\,000$), the cost is not prohibitive; a more detailed discussion of this cost is presented in Appendix C, along with the parts list. Furthermore, the equipment is extremely versatile and can be used for a number of other experiments. By adding approximately $\$2,500$ in components, we have extended the work described here to demonstrate that (i) single photons interfere with themselves as they pass through the two arms of an interferometer, and (ii) that the frequencies of the signal and idler beams generated in our experiment are highly correlated. These experiments will be described in a future publication. With other small additional purchases, it will be possible to perform tests of Bell's inequalities^{9,10} and to demonstrate two-photon interference.^{28,29} Thus, for less than $\$50\,000$, one could implement five experiments suitable for undergraduates that demonstrate interesting features of quantum mechanics. While the total cost is not inexpensive, it is most certainly cost effective.

ACKNOWLEDGMENTS

We wish to acknowledge several helpful discussions with David Branning. We also acknowledge financial support from the National Science Foundation and from Whitman College.

Note added in proof. We have recently become aware that similar experiments have been carried out by a group at Colgate University.³⁰

APPENDIX A: ACCIDENTAL COINCIDENCES

The time interval defining a coincidence is determined by the windowing of the SCAs. Specifically, the SCAs are configured with finite time windows of $\Delta t = 2.5 \text{ ns}$, giving the term "coincidence" the meaning "within 2.5 ns". A consequence of this finite window is a finite probability, proportional to Δt , of registering *GTR* coincidences that have no relation to the coincidences of interest; these are accidental coincidences.

For example, suppose we obtain a valid coincidence between detectors *G* and *T*, which occurs with probability $P_{GT} = R_{GT}/R_G$, where we have written Eq. (13) in terms of the count rates. Within Δt of this coincidence, there is a random chance that the *R* detector also will measure a count, leading to an accidental threefold coincidence. If the time interval Δt is small enough, then the probability of this random *R* detection occurring can be approximated by $P'_R \approx R_R \Delta t$, where the prime indicates that this is an accidental event, occurring within a specific time window. Similarly, a valid *GR* coincidence and a chance detection at *T* also will

yield an accidental threefold coincidence. The probability of the accidental coincidences can then be written as

$$P'_{GTR} = P_{GT}P'_R + P_{GR}P'_T = P_{GT}R_R\Delta t + P_{GR}R_T\Delta t. \quad (18)$$

Here, we have ignored the probability that the accidental threefold coincidences may be due to pure chance detections at all three detectors, because for our count rates and coincidence window, this probability is negligible.

We can now calculate the effect of these accidental coincidences on the second-order coherence. Substituting Eq. (18) into Eq. (12) yields

$$\begin{aligned} g^{(2)}(0) &= \frac{P_{GTR}}{P_{GT}P_{GR}} \\ &= \frac{P_{GT}R_R\Delta t + P_{GR}R_T\Delta t}{P_{GT}P_{GR}} \\ &= \frac{R_R\Delta t}{P_{GR}} + \frac{R_T\Delta t}{P_{GT}} = R_G\Delta t \left(\frac{R_R}{R_{GR}} + \frac{R_T}{R_{GT}} \right). \end{aligned} \quad (19)$$

Using the average count rates obtained from the data collected during trial 4 of Table I, we calculate the contribution to $g^{(2)}(0)$ from the accidental coincidences to be 0.0164.

APPENDIX B: SETTING THE SINGLE-CHANNEL-ANALYZER WINDOW

One technique for setting the voltage window of the SCA is to simply set the window width to some value, and to slowly adjust the lower level of the window while monitoring the SCA output. The goal is to maximize the coincidence rate. The window is then adjusted to be just wide enough so that a further increase in width does not significantly increase the count rate. Adjustments of the width and lower level of the window can be iterated to optimize the count rate.

An easier way to set the SCA window is to use a multi-channel analyzer (MCA). Our MCA is on a PCI card that plugs into our computer and comes with its own software. We use it as a diagnostic tool for setting the window, but do not use it in our experiments to determine $g^{(2)}(0)$. An MCA histograms voltage pulses of varying amplitude. The histogram is displayed in real time, with an update rate of a few hertz, so that one can watch the histogram build over time. The input to the MCA is the output from the TAC, so that the histogram can be interpreted as measuring time intervals instead of voltages. As stated above, coincidence counts at G and T are separated at the TAC by 6 ns, and with the coincidence rates in our experiment, we easily see a peak in the histogram generated by the MCA centered at this 6-ns time delay. The wings of this peak extend outward to a width of approximately 2.5 ns, which is the reason we chose this value for our coincidence window. (This width is due almost entirely to the properties of the SPCMs, as the time interval between the photon pairs produced in our experiment is certainly much less than this.³¹) Uncorrelated photodetections (arising from G seeing a photon from one pair-production event and T seeing a photon from a different pair-production event) contribute a uniform background that the coincidence peak sits on top of.

Simply looking at the output of the TAC on the MCA displays the coincidence peak, but yields no information about the window of the SCA, which is what we are really interested in. In order to set the SCA window, we throw a switch on the TAC/SCA unit, which causes the SCA to win-

now the output of the TAC. In this mode of operation, if the output amplitude of the TAC falls within the voltage window set by the SCA, the TAC operates normally and outputs a voltage proportional to the time difference between the START and STOP pulses. However, if the output of the TAC falls outside of the SCA window, the TAC output is inhibited and there is no TAC output. Thus, if the SCA window is not properly set, no peak appears in the MCA histogram. We thus set the SCA window by simply monitoring the MCA histogram and adjusting the SCA controls until only the coincidence peak is seen and the uncorrelated background is eliminated.

APPENDIX C: PARTS LIST AND COST OF EXPERIMENT

Here, we list the major components for this experiment. A detailed list of all the components can be found on our website.²⁷

Pump Laser: Edmund Industrial Optics, (<http://www.edmundoptics.com/>). Diode-pumped, frequency-doubled, solid-state laser (405–410 nm); model NT55-872; \$5,800.

Downconversion Crystal: Cleveland Crystals, (<http://www.clevelandcrystals.com/>). Beta-barium borate (BBO) crystal, 3 mm long, for converting a cw 405-nm input to an 810-nm output, 3° cone angle on signal and idler, XH0503 housing with a 5-mm aperture, Humidity-barrier antireflective coatings on the crystal faces, nitrogen purge connections, and no windows; \$2,160.

Single-Photon Counting Modules: Pacer Components, (<http://www.pacer.co.uk/>). Single-photon counting module (Perkin Elmer model SPCM-AQR-13-FC), dark count less than 250 cps, FC fiber connector; quantity 3; \$4,300/each.

Counting Electronics: ORTEC, (<http://www.ortec-online.com/>). TAC/SCA model 567; nuclear instruments modular (NIM) plug-in module; quantity 3; \$1,656/each. These modules plug into a NIM crate with associated power supply, which we already had available to us. If a NIM crate is needed, the ORTEC model 4001A/4002D @\$2,500 should be suitable. MCA model TRUMP-PCI-2K (diagnostic for setting up SCA window); PCI plug-in card with software; \$2,370.

Counter: National Instruments, (<http://www.ni.com/>). 8-channel counter/timer model PCI-6602; plug-in card. (Note that the optional BNC-2121 connector block and SH68-68-D1 shielded cable greatly simplify connecting to the counter). Total cost with options, \$1,000.

Alignment Laser and Power Supply: Thorlabs, (<http://www.thorlabs.com/>). 785-nm laser coupled to a single-mode fiber with FC connector; model LPS-4224-785-FC; \$400. ILX Lightwave, (<http://www.ilxlightwave.com/>). Current source model LDX-3412; \$930.

The total cost of the experiment is ~\$40 000. This cost includes all of the equipment necessary to carry out the experiments, with the exception of a computer, LABVIEW software, and the 3×5 foot optical table. The experiment does not require a full optical table—an optical breadboard would be sufficient, and it should be possible to fit everything on a 3×4 ft breadboard. Below, we discuss a few possibilities for reducing the cost of the experiment.

Approximately \$2,500 of the cost is for standard optical components: mirrors, kinematic mounts, posts, etc. A laboratory with a stock of such components could save much of

this cost. The fiber-coupled alignment laser and power supply are nothing special—any available laser coupled into a fiber would suffice.

Another opportunity for reducing cost is in the counting electronics. Many laboratories have some of the necessary electronics as part of existing nuclear physics experiments. Thus, it may be possible to save on the TAC/SCA cost and the cost of a NIM crate. It also is possible to build coincidence counting electronics from integrated circuits,⁹ eliminating nearly \$7,400 in cost.

After our apparatus was assembled, Perkin Elmer introduced the SPCM-AQ4C, which consists of four fiber-coupled photon-counting modules in one unit. These modules have a larger dark count rate (500 cps), but that should have little or no effect on the experiments described here. The cost of this unit is \$9,000, which is significantly cheaper than purchasing three separate counters. If we were building a new system, we would use this unit.

We do not recommend replacing the avalanche photodiode-based photon-counting modules with photomultiplier tubes (PMTs). Quantum efficiencies of most PMTs above 800 nm are about 100 times smaller than avalanche photodiodes, meaning that the count rates would be 100 times lower. PMTs with GaAs photocathodes have efficiencies that are only 5 or 6 times lower than avalanche photodiodes, which is not too bad. However, PMT-based systems further require the use of cooled housings, high-voltage (HV) power supplies, discriminators, and possibly high speed amplifiers; this increases the cost and complexity of PMT-based systems. Even PMT-based photon-counting modules (which incorporate the housing, HV supply, and discriminator) operate significantly better with external temperature control circuitry, which makes their cost higher than the avalanche diode systems.

If a high-compliance voltage laser diode current source is already available, stand-alone 30 mW blue laser diodes are available directly from Nichia, (www.nichia.com), for \$2,000 each. It would be advisable to have a temperature-controlled mount for this diode. If a laboratory already has an Ar-ion laser, it could be used. The bluest line with significant power (10 s of mW) is typically at 458 nm, which places the downconversion at 916 nm. There is a slight reduction in quantum efficiency of the avalanche diodes at this wavelength, but we envision no significant obstacles to operating at this wavelength.

^aElectronic mail: beckmk@whitman.edu

¹R. Q. Stanley, "Question #45: What (if anything) does the photoelectric effect teach us?," *Am. J. Phys.* **64**, 839 (1996).

²P. W. Milonni, "Answer to Question #45: What (if anything) does the photoelectric effect teach us?," *Am. J. Phys.* **65**, 11–12 (1997).

³W. E. Lamb, Jr. and M. O. Scully, "The photoelectric effect without photons," in *Polarization, Matière et Rayonnement* (Presses University de France, Paris, 1969).

⁴L. Mandel, "The case for and against semiclassical radiation theory," in *Progress in Optics*, edited by E. Wolf (North-Holland, Amsterdam, 1976), Vol. XIII, pp. 27–68.

⁵D. C. Burnham and D. L. Weinberg, "Observation of simultaneity in para-

metric production of optical photon pairs," *Phys. Rev. Lett.* **25**, 84–87 (1970).

⁶J. F. Clauser, "Experimental distinction between the quantum and classical field-theoretic predictions for the photoelectric effect," *Phys. Rev. D* **9**, 853–860 (1974).

⁷H. J. Kimble, M. Dagenais, and L. Mandel, "Photon antibunching in resonance fluorescence," *Phys. Rev. Lett.* **39**, 691–695 (1977).

⁸A. C. Funk and M. Beck, "Sub-Poissonian photocurrent statistics: Theory and undergraduate experiment," *Am. J. Phys.* **65**, 492–500 (1997).

⁹D. Dehlinger and M. W. Mitchell, "Entangled photon apparatus for the undergraduate laboratory," *Am. J. Phys.* **70**, 898–902 (2002).

¹⁰D. Dehlinger and M. W. Mitchell, "Entangled photons, nonlocality, and Bell inequalities in the undergraduate laboratory," *Am. J. Phys.* **70**, 903–910 (2002).

¹¹P. Grangier, G. Roger, and A. Aspect, "Experimental evidence for a photon anticorrelation effect on a beam splitter: A new light on single-photon interferences," *Europhys. Lett.* **1**, 173–179 (1986).

¹²G. Greenstein and A. G. Zajonc, *The Quantum Challenge, Modern Research on the Foundations of Quantum Theory* (Jones and Bartlett, Sudbury, MA, 1997).

¹³R. Hanbury Brown and R. Q. Twiss, "Correlation between photons in two coherent beams of light," *Nature (London)* **177**, 27–29 (1956).

¹⁴An excellent compilation of reprints, including many of the articles referenced here, is L. Mandel and E. Wolf, *Selected Papers on Coherence and Fluctuations of Light (1850–1966)* (SPIE, Bellingham, WA, 1990).

¹⁵R. Hanbury Brown and R. Q. Twiss, "A test of a new type of stellar interferometer on Sirius," *Nature (London)* **178**, 1046–1048 (1956).

¹⁶E. Brannen and H. I. S. Ferguson, "The question of correlation between photons in coherent light rays," *Nature (London)* **178**, 481–482 (1956).

¹⁷E. M. Purcell, "The question of correlation between photons in coherent light rays," *Nature (London)* **178**, 1449–1450 (1956).

¹⁸R. Hanbury Brown and R. Q. Twiss, "Interferometry of the intensity fluctuations in light I. Basic theory: the correlation between photons in coherent beams of radiation," *Proc. R. Soc. London, Ser. A* **242**, 300–324 (1957).

¹⁹R. Q. Twiss, A. G. Little, and R. Hanbury Brown, "Correlation between photons in coherent beams of light, detected by a coincidence counting technique," *Nature (London)* **180**, 324–326 (1957).

²⁰R. Loudon, *The Quantum Theory of Light*, 3rd ed. (Clarendon, Oxford, 2000).

²¹A way to motivate the validity of this inequality is to note that the variance of the intensity must be a positive number. Since the variance can be written as $\Delta I^2 = \langle I^2 \rangle - \langle I \rangle^2 \geq 0$, it must be true that $\langle I^2 \rangle \geq \langle I \rangle^2$.

²²F. T. Arecchi, E. Gatti, and A. Sona, "Time distribution of photons from coherent and Gaussian sources," *Phys. Lett.* **20**, 27–29 (1966).

²³L. Mandel and E. Wolf, *Optical Coherence and Quantum Optics* (Cambridge U.P., Cambridge, 1995).

²⁴P. L. Kelly and W. H. Kleiner, "Theory of electromagnetic field measurement and photoelectron counting," *Phys. Rev.* **136**, A316–A334 (1964).

²⁵R. J. Glauber, "Optical coherence and photon statistics," in *Quantum Optics and Electronics*, edited by C. DeWitt-Moretz, A. Blandin, and C. Cohen-Tannoudji (Gordon and Breach, New York, 1965), pp. 63–185.

²⁶Z. Y. Ou, C. K. Hong, and L. Mandel, "Relation between input and output states for a beamsplitter," *Opt. Commun.* **63**, 118–122 (1987).

²⁷<http://www.whitman.edu/~beckmk/QM/>

²⁸C. K. Hong, Z. Y. Ou, and L. Mandel, "Measurement of subpicosecond time intervals between two photons by interference," *Phys. Rev. Lett.* **59**, 2044–2046 (1987).

²⁹C. H. Holbrow, E. Galvez, and M. E. Parks, "Photon quantum mechanics and beamsplitters," *Am. J. Phys.* **70**, 260–265 (2002).

³⁰E. J. Galvez *et al.*, personal communication, 2004.

³¹S. Friberg, C. K. Hong, and L. Mandel, "Measurement of time delays in the parametric production of photon pairs," *Phys. Rev. Lett.* **54**, 2011–2013 (1985).

Lab 1:

Spontaneous Parametric Downconversion

Lab Ticket -- must be finished before you come to lab. Each group turns in one ticket.

You have a nonlinear crystal which has been cut to downconvert light at 405 nm to signal and idler beams at 810 nm. If the index of refraction of the crystal is 1.659 at 405nm, and 1.661 at 810nm, what angle do the signal and idler beams make with respect to the pump?

Important Safety Tips

- For your safety, **NEVER LOOK DIRECTLY INTO THE LASER.** You should **WEAR THE LASER SAFTY GOGGLES** while in the lab; they will block the intense blue laser light, but still allow you to see.
- **REMOVE YOUR WATCH OR ANY OTHER SHINY JEWELRY THAT'S ON YOUR HANDS OR WRISTS.** A reflection off of a shiny surface can be accidentally directed to someone's eye.
- For the safety of the equipment, **NEVER TURN ON THE ROOM LIGHTS WHILE THE PHOTON COUNTING MODULES ARE ON.**

There is a small box on the table that has a 3-position switch on it. These boxes are connected to the single photon counting modules (SPCM's). The switch positions are labeled "OFF", "GATE" and "ON" (or just "OFF" and "ON"). **This switch must be in the OFF position when the room lights are on.** There is a separate switch to turn on the power to the modules; it is OK for the power to be on, but the detectors themselves must be OFF.

- In general, if the manual is not clear, or you're not completely sure how to do something, **PLEASE ASK FOR HELP.**

While in the Lab

You should have some sort of notebook to write things down while you are in the lab. You will notice that there may be questions you will be asked to answer in the course of these laboratories. You will not have time to answer all of these questions while in the lab, but you should record all of the necessary observations that you will need in order to answer them. Your time in the lab is limited; make and record observations in the lab, but perform calculations when the lab is over.

It will also be helpful for you to record in your notebook the names of the data files you generate, along with the parameters you used and the key results you obtained. It can be quite frustrating to know that you have a good data set, but not remember which one it is, or what parameters you used to obtain it.

I. Introduction

All of the experiments that you will perform this semester will be based on the process of spontaneous parametric downconversion. This physical process comes in many variations, but at its most basic level it is a process in which light of one frequency is converted into light of a different frequency. Any optical process which changes the frequency of a light beam is inherently *nonlinear*. Most of the other optical processes you are probably familiar with (absorption, reflection, refraction, polarization rotation, etc.) are *linear* processes; they may affect many properties of a light field, but linear processes can never change the frequency of light.

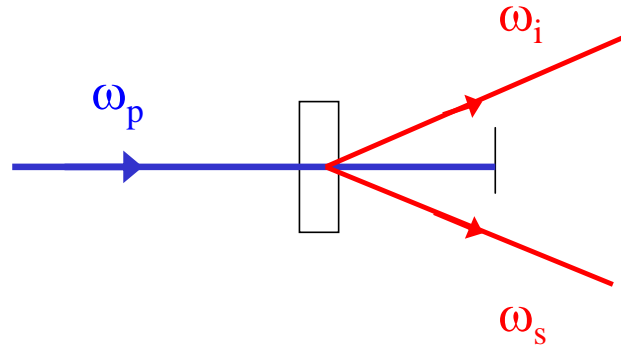


Fig. 1 Spontaneous parametric downconversion.

In the process of spontaneous parametric down conversion, shown schematically in Fig. 1, a single photon of one frequency is converted into two photons of lower frequency (by approximately a factor of 2) in a nonlinear crystal. While downconversion is extremely inefficient (10's of milliwatts of input power generate output beams that must be detected using photon counting) it is much more efficient than other sources of photon pairs (for example, atomic emission of 2 photons).

The input wave is referred to as the pump (at angular frequency ω_p), while the two outputs are referred to as the signal and idler (at angular frequencies ω_s and ω_i). This process is said to be "spontaneous" (as opposed to "stimulated") because there are no input signal and idler fields, they're generated spontaneously from the pump in the crystal. The process is "parametric" because it depends on the electric fields, and not just their intensities. This means that there is a definite phase relationship between the input and output fields. It is called "downconversion" because the signal and idler fields are at a lower frequency than the pump field.

Energy conservation requires that

$$\begin{aligned}\hbar\omega_p &= \hbar\omega_s + \hbar\omega_i \\ \omega_p &= \omega_s + \omega_i .\end{aligned}\tag{1}$$

Momentum conservation is equivalent to a classical condition known as "phase-matching", which requires that the wave vectors of the input and output fields satisfy

$$\vec{k}_p = \vec{k}_s + \vec{k}_i .\tag{2}$$

The frequencies and wave-vectors are not independent of each other, and are related by the dispersion relationship

$$k_p = \frac{n_p(\omega_p)\omega_p}{c} ,\tag{3}$$

where $n_p(\omega_p)$ is the index of refraction of the pump wave at the pump frequency, and similarly for the signal and idler waves.

In type I downconversion, which is what we will use in our experiment, the signal and idler beams are polarized parallel to each other, and their polarization is perpendicular to that of the pump; all polarizations are linear. By proper orientation of the pump beam wavevector \vec{k}_p with respect to the optic axis of the crystal, it is possible to satisfy the constraints imposed in Eqs. (1)-(3).

The crystal we use is beta-Barium Borate (BBO). In our experiments the pump laser has a wavelength of around 405nm, while the signal and idler beams are at 810nm (twice the wavelength, half the frequency). In order to separate signal and idler, they are chosen to make a small angle (a few degrees) with the pump beam; so the signal comes out a few degrees from the pump, and the idler comes out a few degrees on the other side of the pump. Since only the relative angles between the pump, signal and idler are important, the signal and idler beams are emitted into cones surrounding the pump beam (see, for example, Ref. 1).

However, for a given crystal orientation, there is not a unique solution to the constraints imposed in Eqs. (1)-(3). The sums of the frequencies and wavevectors are constrained, but not the individual frequencies and wavevectors. As shown in Fig. 2, if the idler frequency is somewhat more than half the pump frequency, it is possible for energy to be conserved, Eq. (1), if the signal frequency is an equal amount less. In order for momentum to be conserved, Eq. (2), the signal then makes a slightly greater angle with respect to the pump, and the idler makes a slightly less angle. Thus, the light coming out of a down conversion crystal is emitted into a range of angles (several degrees), and wavelengths (on the order of 10's of nm, centered about twice the pump wavelength.)

The experimental apparatus is shown in Fig. 3. The signal and idler photons are collected with lenses, coupled into optical fibers and directed to single photon counting modules (SPCM's) where they are detected. Not shown in this figure are colored glass filters, which are in-line with the fibers, between the collection lenses and the SPCM's. These are RG780 filters that block wavelengths shorter than 780nm, and transmit wavelengths longer than this. Their purpose is to

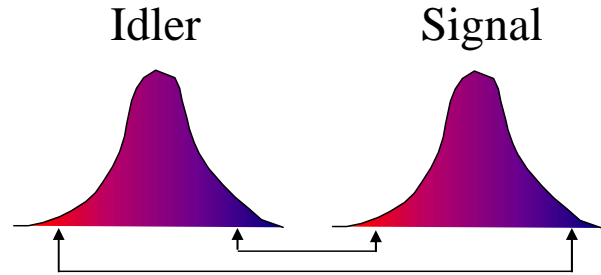


Fig. 2 Correlations between the frequencies of the signal and idler beams. If the idler frequency increases, the signal frequency decreases, and vice versa.

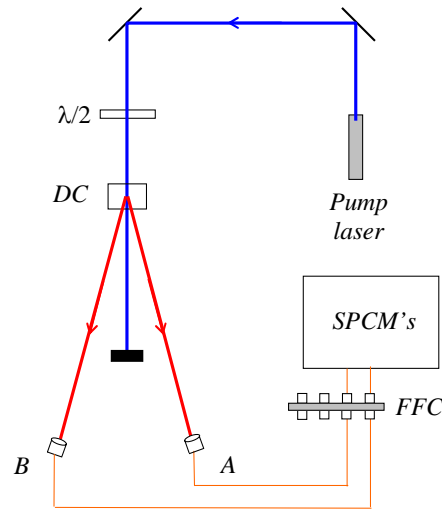


Fig. 3 The experimental arrangement. Here $\lambda/2$ denotes a half-wave plate, DC denotes the downconversion crystal, FFC denotes fiber-to-fiber coupler, and SPCM's denotes the single photon counting modules,

transmit the downconverted light, while blocking scattered blue pump light, and the green light we use to illuminate the laboratory.

The most crucial aspect of the experiment is properly coupling the signal and idler beams into the fibers, and maximizing the number of coincidence counts obtained between the signal and idler beams. The alignment of the idler beam into the A-detector will be done for you before you start, so your first task is to align the B-detector with the signal beam.

We speak of aligning the B-detector, but really we mean aligning the lens and optical fiber that deliver the downconverted light to the detector. Shown in Fig. 4 are the mounts, lenses and fibers for this experiment. The bases which hold the mounts slide along a ruler, which is fastened to the table. This allows reasonably precise translation of the mounts, in order to position them at the correct angles to detect the downconverted photons. The downconversion crystal we will use is cut so that the signal and idler beams make nominal 3° angles with respect to the pump beam.

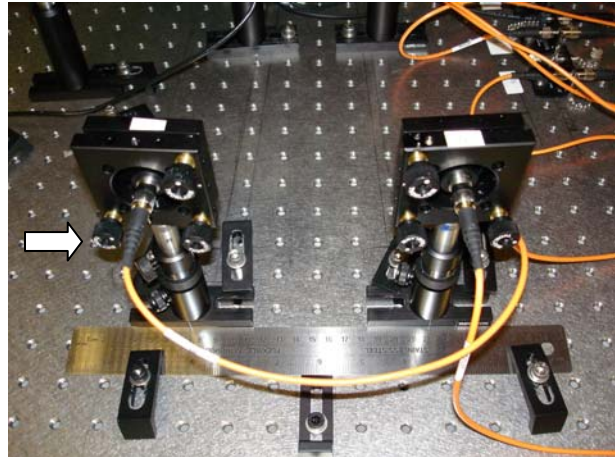


Fig. 4 View from the back side of the mounts, lenses and fibers which collect the downconverted light. The ruler is used to help position things. The green arrow shows the knob you use to adjust the horizontal tilt of the B-detector.

II. Getting Started

- Please wait for me to show you how to turn things on, etc.
- Make sure the coincidence circuit is set to “G2” and 10Hz.
- Start by double-clicking the “Coincidence.vi” icon on your desktop.

This launches LabView and loads the data acquisition program. Documentation for the program is given in Appendix A.

- Run the program by clicking the Run icon (the arrow in the upper left corner of the window.)
- If you ever need to stop the program, do so by pushing the **STOP** button in the upper left. Do not simply close the window without stopping -- if you do this the program does not exit gracefully. At the very least you'll need to restart LabView; you may need to reboot the machine.

After a few seconds the program is running, reading the counters, and updating the screen in real time--although this may not be obvious at first because the detectors should still be turned off.

- Make sure the room lights are turned off (it's OK for the green safe flights to be on) and turn on the detectors.

Now the indicators on the screen should be changing, and it should be more obvious that the program is running. The mode the program is currently running in is useful for "tweaking": adjusting the various parameters and seeing how they affect the measured count rates. Once things are adjusted how you want them to be, you press the **Take Data** button and the program switches to data record mode, where the data is saved to a file on the disk.

- Make sure the **Experimental Setup** dial is set to **Coincidence** (if it isn't, click on the dial and rotate it), and that **Update Period** is set to 0.2s (if it isn't, highlight the value, type "0.2", and hit <Enter>).

You should see a large number of **A** counts. You'll probably see a small number of **B** counts, and no **AB** coincidence counts.

III. Detector Alignment

The idea now is to place the **B** detector in the proper location to maximize the number of **AB** coincidence counts. Remember that although the downconverted light is emitted in many directions, individual pairs of photons have well defined angles, as determined by Eq. (2). Since the **A** detector is fixed, it is necessary to place the **B** detector in the correct spot to detect the pair photons.

- Place the **B** detector mount so that the base pushes the up against the ruler, as shown in Fig. 4. Begin by locating the **B** detector so that it makes roughly the same angle from the pump beam as the **A** detector.
- While holding the mount in place with one hand, use your other hand to adjust the horizontal tilt so that the detector is looking straight back at the downconversion crystal. Use the knob shown in Fig. 4 to do this while you monitor the **AB** coincidences; the goal is to maximize these coincidences.
- Once you've got things properly adjusted, carefully let go of the mount, trying to maintain the alignment. Use the chart to estimate the average **AB** coincidence rate. In your notebook record the position of the detector (using the ruler as a guide) and the coincidence rate.
- Slide the detector 1 or 2 mm in either direction, and readjust the tilt to maximize the **AB** coincidence rate. Again record the position and the rate.
- Continue to move and tilt the detector until you find an alignment which maximizes the coincidence count rate. You shouldn't have too much trouble obtaining a maximum coincidence rate of 1000 cps (counts-per-second -- note the units) or better.

Having done the above you should have the optimal alignment, and some idea of the range over which you can obtain coincidences. Now it's time to make a careful study of how the coincidence rate depends on angle. Start by calculating the angle that the signal beam makes with the pump beam when the **B** detector is optimally aligned. You will scan over a 1° range of angles, centered about the optimal angle. I would like you to take at least 10 data points across this range, calculating the average and standard deviation of the coincidence rate at each point. You will use the **Take Data** feature of the program to do this.

- Place the detector so that it is at the smallest angular position you will acquire data at, and adjust the tilt to optimize the coincidence rate.
- In the **Data Taking Parameters** section of the program set **Update Period (Data Run)** to 1.0s, and **Number of Points** to 10. Now press the **Take Data** button.

A new window will automatically open as the computer switches to data taking mode. The computer will automatically take 10 measurements with 1.0s counting windows, plot the data on the screen, calculate the mean and standard deviation of the coincidence rate, and save all the data to a file. The data file is automatically named according to the date and time.

- In your notebook record the filename, important parameters (e.g., the location of the detector), and the results.
- Once you have written down all of these parameters, you can close the window of the data recording program.
- Check the data file you just created . There is a shortcut to the Data folder on your desktop. Inside the Data folder find the folder with today's date on it, and your file should be in there. Open it up and look at it (it's easiest to use Excel—right click on the file and choose “Open With” Excel); the info in the file should agree with what you wrote in your notebook. Despite the fact that most of this information is stored in the computer (it doesn't know the detector position, for example), the notebook is handy because you can easily find the names of the good data sets, and don't have to open lots of files to find what you're looking for.

When you are all done with the lab, remember to save all your data on your network drive. I suggest you use the Web version of Netfiles.

- Repeat the above process for at least 10 data points over a 1° range of angles. At the two extremes of your data, the coincidence rates should be less than 10% of the maximum rate; if this is not the case you should take more data at larger angles.
- When you're all done taking data, place your detector at the optimum position, and lock it to the table with the clamps.

After you leave the lab create a graph of coincidence count rate versus angle, including error bars.

- ◆ **Q1: Approximately what is the full width at half maximum (FWHM) of this distribution?**

IV. Timing

The photon pairs are produced not only with well defined angles, but also at well defined times. Indeed, the two photons are produced at the same time. We can't say that they are produced at *exactly* the same time, because, as you will learn in class, there is an uncertainty relationship between energy and time. For our experimental parameters the uncertainty in time is on the order of 10fs -- a time that is much shorter than our experimental apparatus can resolve. Here we will be able to show that this uncertainty is less than a nanosecond.

In order to perform this measurement you'll use an instrument known as a Time-to-Amplitude Converter (TAC), which measures the time interval between two events. In our case

the two events are the detections of two photons. One detector is connected to the START input of the TAC, while the other is connected to the STOP input. The TAC outputs a voltage pulse whose height is proportional to the time interval between these events. We ensure that the STOP always comes after the START by inserting an extra length of electrical cable between the STOP detector and the TAC. We will thus measure a time interval that is offset from zero by this electrical delay; we are not interested in this offset, but rather in the width of the distribution of the arrival times.

The output pulses from the TAC are most easily analyzed with an instrument known as a multi-channel analyzer (MCA). An MCA reads in the voltage pulses and displays a histogram of the pulse heights. Because we can calibrate the TAC, this is essentially a measurement of the distribution of time intervals.

- Find me so I can help you in hooking the detectors up to the TAC.
- Double-click the “MCA.vi” icon on your desktop, and then run it by clicking the arrow. Documentation for this program is given in Appendix C. Note that MCA.vi and Coincidence.vi can both be open at the same time, but they cannot both be running at the same time.
- This program updates the screen after a certain number of pulses are measured, not after a certain time interval. So, if nothing happens after a few seconds it probably means that there are no voltage pulses present. Make sure that the lights are off, and the detectors are on.
- You should see a sharp peak appear in the distribution on your screen. Place the cursors on either side of this peak, then click **Zoom to Cursors** to zoom in on it.
- Click the **Clear Buffer** button to see what it does.
- Hit the **Clear Buffer** button, accumulate some data so that you can clearly see the peak. Push the **Save Data** button to save the data to a file.

After you leave the lab, create a graph displaying this data. Turn this graph in with your lab report. Don't necessarily show all the data, but show about a 10 ns window around the coincidence peak.

- ◆ Q2: Approximately what is the full width at half maximum (FWHM) of this distribution?
- ◆ Q3: How wide a time window would you need to count essentially all of the coincidences, but as little as possible of the background?
- ◆ Q4: Our coincidence circuit has a coincidence window of about 8 ns (assume it's centered about the peak). Given this information, estimate what fraction of the coincidences that are measured are true coincidences, and what fraction are “accidental” coincidences due to the background. Explain how you came up with this estimate.

V. Write-up

Your write-up should include:

- Answers to all questions.

- A brief (less than one page) write-up describing what you did in the lab, and summarizing your results. In your report I'd like you to discuss the resolution of the measurements. What do you think limits the width of the coincidence peaks--both in angle and in time?
- Graphs of your data.

References:

- [1] D. Dehlinger and M. W. Mitchell, "Entangled photons, nonlocality, and Bell inequalities in the undergraduate laboratory," *Am. J. Phys.* **70**, 903-910 (2002).

Lab 2:

Proof of the Existence of Photons

Lab Ticket -- must be finished before you come to lab. Each group turns in one ticket.

Read Ref. [2] -- at least the introduction and theory sections.

Using the expression for $g^{(2)}(0)$ in terms of experimentally measurable quantities, explain why we hope to measure $g^{(2)}(0)=0$ in the single-photon experiment.

Important Safety Tips

- For your safety, **NEVER LOOK DIRECTLY INTO THE LASER.** You should **WEAR THE LASER SAFETY GOGGLES** while in the lab; they will block the intense blue laser light, but still allow you to see.
- **REMOVE YOUR WATCH OR ANY OTHER SHINY JEWELRY THAT'S ON YOUR HANDS OR WRISTS.** A reflection off of a shiny surface can be accidentally directed to someone's eye.
- For the safety of the equipment, **NEVER TURN ON THE ROOM LIGHTS WHILE THE PHOTON COUNTING MODULES ARE ON.**

There is a small box on the table that has a 3-position switch on it. These boxes are connected to the single photon counting modules (SPCM's). The switch positions are labeled "OFF", "GATE" and "ON" (or just "OFF" and "ON"). **This switch must be in the OFF position when the room lights are on.** There is a separate switch to turn on the power to the modules; it is OK for the power to be on, but the detectors themselves must be OFF.

- In general, if the manual is not clear, or you're not completely sure how to do something, **PLEASE ASK FOR HELP.**

I. Introduction

First we should define what we mean by "proving" photons exist. Classically, light is an electromagnetic wave. Quantum mechanically, light has both wave-like and particle-like properties, and the quanta are called photons. So, to prove that light is made of photons you want to do an experiment which makes this granular nature of the field apparent.

However, this is not enough. We never measure light directly, but always measure the current from a detector instead. It is possible for the granularity of our measurements to be caused by the discrete nature of the electrons in our detector. Assume a classical wave is incident on a detector. How do we determine whether the granularity of our measurements is due to the discreteness of electrons in the detector, or the discreteness of photons in the field? There is no easy way to do this. Observing granularity in measurements of a field is a necessary,

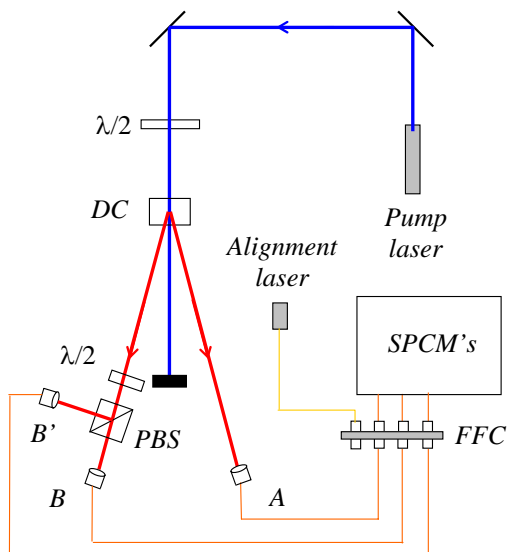


Fig. 1. The experimental apparatus. In addition to the pieces of equipment introduced in the last lab, here we have a polarizing beamsplitter (PBS).

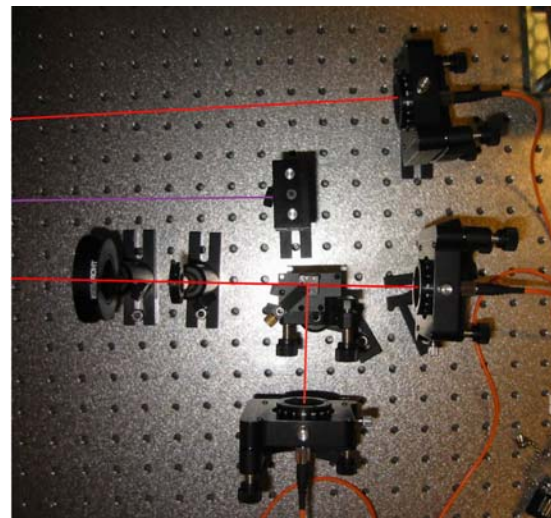


Fig 2. Picture showing the waveplate, PBS, and the collection optics. Beam paths are shown for clarity.

but not a sufficient, condition for the existence of photons. Granularity motivates the existence of photons, but does not prove it.

Since photons are inherently a quantum mechanical object (remember, classical waves aren't made of photons), an experiment which requires a quantum mechanical explanation would imply that the field is made of photons. In other words, if we do an experiment that we cannot explain classically, it means there is more to the field than just classical waves. To be precise, the experiment we will do distinguishes between quantum mechanical and classical theories of the electromagnetic field. If classical waves cannot explain the results, then we take this to mean that photons exist.

You will be performing an updated version of the experiment performed originally by Grangier, Roger and Aspect [1-3]. The experimental apparatus is shown in Figs. 1 & 2. The basic idea is to show that if a single photon is incident on the beamsplitter, it can be detected at **B**, or at **B'**, but not both. We ensure that a single photon is incident on the beamsplitter by conditioning all of the measurements on a detection at **A**.

The measurements are quantified using a parameter called the degree of second-order coherence, $g^{(2)}(0)$. Instead of repeating here what's already been written elsewhere, you should read Ref. [2], which provides the theoretical background for this experiment. In that article you'll learn that a classical wave theory requires $g^{(2)}(0) \geq 1$. This is an instance of a classical inequality, of which there are many in physics. There are situations in which quantum mechanics can violate classical inequalities, and in these cases we say that we are observing strictly quantum mechanical phenomena. For this experiment, if we measure a value of $g^{(2)}(0) < 1$, then the field cannot be explained classically, and we have proven the existence of

photons. The quantum state which yields maximum violation of this classical inequality is the single photon state, for which the quantum prediction is $g^{(2)}(0)=0$.

The above described experiment uses three detectors to measure $g^{(2)}(0)$. I look at this as measuring $g^{(2)}(0)$ for the signal beam striking the beamsplitter, *conditioned* on a detection in the idler beam. The conditioning is key -- it's what prepares the signal beam in a single photon state. Without this conditioning the beam striking the beamsplitter is purely classical. To prove this you will also perform a two-detector, unconditional measurement of the signal beam, for which you should observe $g^{(2)}(0)\geq 1$.

II. Theory

There's a lot of detailed the theory in Ref. [2], especially on the three-detector measurements. However, there's not much information there on two-detector measurements, so I'll give some detail on that here.

Lets start with the two-detector theory. When $g^{(2)}(0)$ is measured using photoelectric detection, it can be written in terms of the probabilities of individual photodetections as

$$g^{(2)}(0) = \frac{P_{BB'}}{P_B P_{B'}} \quad (2\text{-detector}), \quad (1)$$

where P_B ($P_{B'}$) is the probability of a detection at detector **B** (**B'**) in a time interval Δt , and $P_{BB'}$ is the probability of making detections at both **B** and **B'** in the same time interval (i.e., a coincidence detection). We can express the probabilities in terms of measured count rates. For example, the probability of a detection at **B** in a short time interval Δt is simply given by the average rate of detections, multiplied by Δt . The average rate of detections at **B** is just the number of detections N_B divided by the counting time T that we are averaging over. The probabilities for **B** detections and **BB'** coincidences are given similarly:

$$P_B = \left(\frac{N_B}{T}\right)\Delta t, \quad P_{B'} = \left(\frac{N_{B'}}{T}\right)\Delta t, \quad P_{BB'} = \left(\frac{N_{BB'}}{T}\right)\Delta t \quad (2)$$

Substituting this into Eq. (1), we get

$$g^{(2)}(0) = \frac{N_{BB'}}{N_B N_{B'}} \left(\frac{T}{\Delta t}\right) \quad (2\text{-detector}). \quad (3)$$

For measuring the conditional $g^{(2)}(0)$ using three detectors, all of our probabilities are further conditioned upon a detection at **A**. In this case we have [in place of Eq. (1)]

$$g^{(2)}(0) = \frac{P_{ABB'}}{P_{AB} P_{AB'}} \quad (3\text{-detector}), \quad (4)$$

where $P_{ABB'}$ is the probability of threefold detection. Since we are not interested in any events unless detector **A** fires, the number of detections at **A**, N_A , serves as the number of trials which we can use to normalize our probabilities:

$$P_{AB} = \frac{N_{AB}}{N_A}, \quad P_{AB'} = \frac{N_{AB'}}{N_A}, \quad P_{ABB'} = \frac{N_{ABB'}}{N_A} \quad (5)$$

Using these probabilities $g^{(2)}(0)$ for the three-detector measurements becomes

$$g^{(2)}(0) = \frac{N_A N_{ABB'}}{N_{AB} N_{AB'}} \quad (3\text{-detector}). \quad (6)$$

This is the expression from Ref. [2].

III. Getting Started

In Lab 1 you maximized the coincidence count rate between detectors **A** and **B**. When you come into the lab, that much of the alignment will already have been done. Your task this week will be to insert a beamsplitter in the signal beam, and to align detector **B'**. Once this is done you'll be able to measure $g^{(2)}(0)$, and show that light is made of photons.

- Please wait for me to show you how to turn things on, etc.
- Make sure the coincidence circuit is set to “G2” and 10Hz.
- Double-click the “Coincidence.vi” icon on your desktop, and then click the arrow in the upper left corner to run the program.
- Set **Experimental Setup** to **g(2)(0) 3-det**, and **Update Period** to 0.2s. In the pane that displays the graphs, choose the **AB & AB'** tab.
- The **ABB' Coincidence Window (ns)** parameter tells the computer the effective time window for the three-fold coincidence determination. In three-detector measurements this parameter is needed to calculate the expected value for $g^{(2)}(0)$. Ask your instructor for the precise value; it should be on the order of 5-10 ns for the coincidence circuit we're using.
- Make sure that the lights are out, and then turn on the detectors. You should notice more than 1000 **AB** coincidences per second; if you don't, ask for help.
- There are iris diaphragms in the signal beam; they have been placed there to define the path of this beam. You can open and close these diaphragms by rotating the lever on the top. Try doing this while you observe the coincidence rate. You should be able to close the irises to a diameter of about 2mm without affecting this count rate. If this isn't the case, ask for help.
- **Turn off the detectors.**

IV. Aligning the Beamsplitter

Before going on to the next step, make sure I have shown you how to connect fibers to the fiber-fiber coupler, and how to use the alignment laser.

- **Make sure the detectors are off.**

- The fiber from the **B** collection optics leads to a fiber-fiber connector, where it joins another fiber which leads to the filters and a SPCM. Unscrew the fiber coming from the **B** collection optics, and connect it instead to the fiber leading from the alignment laser, as shown in Fig. 3. **Take care when you do this.**

- Turn on the alignment laser (**maximum current of 55 mA**), and light from this laser will shine backward through the **B**-fiber and emerge as a collimated beam from the fiber coupling lens attached to the end of the fiber; see Fig. 3.* The laser light appears dim because it is at a wavelength your eye is not very sensitive to. If you stick white paper in the beam you should

be able to see it with the room lights out. You should be able to see it very brightly using the CCD camera and TV monitor. If the laser light is not shining backwards through the two irises and onto the downconversion crystal, ask for help.

- Insert the polarizing beamsplitter (PBS) about 3-4 inches away from the **B** collection optics (Fig. 2). Make sure it is oriented so that light coming from the downconversion crystal will be reflected toward the edge of the table. Make sure that the beam passes through the center of the beamsplitter.
- Orient the beamsplitter so that its face is perpendicular to the beam. Do this by using the CCD camera to look at the back-reflection from the beamsplitter, which shines back toward the collection optics. Orient the beamsplitter so that this back-reflection goes straight back on top of the incident beam. Screw the beamsplitter mount to the table.
- Insert the half-waveplate an inch or two in front of the beamsplitter. Again, center it, orient it perpendicular to the beam, and screw it to the table.

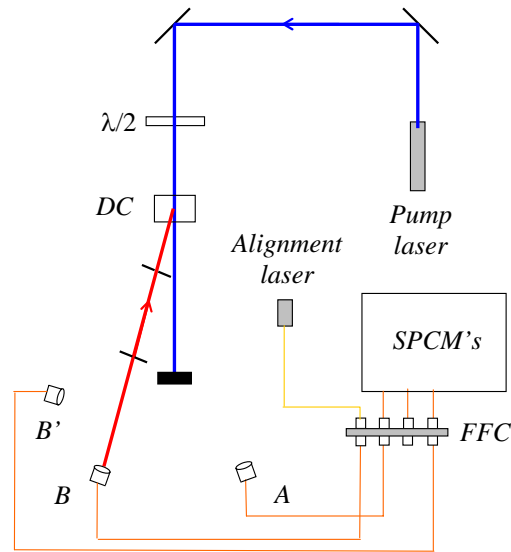


Fig. 3. Using the alignment laser. It should travel backwards from the collection optics, through the irises, and onto the downconversion crystal.

*The alignment laser puts out several mW of light at about 780nm. Your eye is not very sensitive to this light, but it IS a fairly intense beam, and you should **be very careful not to look directly into it. Also, take care not to accidentally couple the laser light into the fiber leading to the SPCM's.** The filters will not block much light at this wavelength, and the SPCM's are VERY sensitive to it and could easily be damaged. It is wise to **make sure that the SPCM's are turned off while the alignment laser is turned on.**

V. Aligning the B' Detector

The next part of the laboratory is probably the most difficult. You will be aligning the **B'** detector so that it collects light from the same beam as the **B** detector. The better job you do aligning this detector, the more light you will collect, the higher your signal-to-noise ratio will be, and the better the results you will obtain.

- Place the mount with the **B'** collection optics on the reflection side of the beamsplitter, about an equal distance from the beamsplitter as the **B** collection optics (Fig. 2). Don't screw it down yet.
- Unscrew the **B**-fiber from the alignment laser, and reconnect it to the fiber leading to the detector. Connect the **B'**-fiber to the alignment laser, as shown in Fig. 4. At this point the beam won't go back through the irises.
- The task now is to get the alignment laser to shine back through the irises and onto the downconversion crystal. By moving the mount sideways (perpendicular to the beam), rotating it, and adjusting the vertical tilt, position it as well as you can to shine the light back through the two pinholes. The CCD camera will be helpful for this. It won't be perfect, but the better job you do on this course alignment, the easier the fine alignment will be. Once you've got it coarsely aligned, screw it to the table.
- Adjust the vertical and horizontal tilt of the **B'** collection optics to perfectly center the beam on the iris closest to the beamsplitter.
- Adjust the vertical and horizontal tilt of the beamsplitter to center the beam on the iris closest to the downconversion crystal.
- Alternate back and forth between the last two steps, always adjusting the collection optics to center the beam on the first iris, and the beamsplitter to center the beam on the second. When the beam is well centered on both irises, you're done.
- **Turn off the alignment laser.**
- Unscrew the **B'**-fiber from the alignment laser, and reconnect it to the fiber leading to the detector.

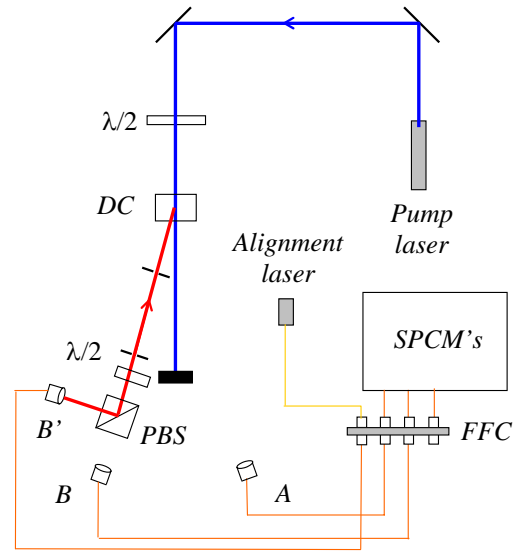


Fig. 4. Aligning the B' detector.

VI. Measuring $g^{(2)}(0)$ for a Single Photon State

- Make sure that the room lights and the alignment laser are off, and then turn on the detectors. Open the iris diaphragms.
- Slowly rotate the waveplate in front of the beamsplitter while monitoring the count rates. You should notice that for some waveplate angles you get lots of **B** and **AB** counts, but

almost no **B'** and **AB'** counts. For other angles you get lots of **B'** and **AB'** counts, but almost no **B** and **AB** counts.

- Rotate the waveplate to maximize the **AB** counts. Adjust the tilt on the **B** mount to maximize this count rate.
- Rotate the waveplate to maximize the **AB'** counts. Adjust the tilt on the **B'** mount to maximize this count rate.
- The maximum **AB** and **AB'** count rates should be nearly the same (within 10 or 20%). If this isn't the case, please ask for help.
- ♦ **Q1: When the waveplate is set to 0°, are the **B** or **B'** counts maximized? How far do you have to rotate the waveplate in order to maximize the other count rate? Explain why the count rates change the way they do when the waveplate is rotated.**
- ♦ **Q2: The polarizing beamsplitter reflects vertically polarized light, and transmits horizontally polarized light. What polarization is the light emerging from the downconversion crystal?**
- Rotate the waveplate to roughly equalize the **AB** and **AB'** count rates. The **AB' minus AB** meter is useful for this.
- Increase **Update Period** to 1s.

You should notice that there are very few **ABB'** threefold coincidences.

- In the pane with the plots, click on the **g⁽²⁾(0)** tab. In the pane labeled **g⁽²⁾ Measurements**, click **Clear Buffer**.

The $g^{(2)}(0)$ measurements will fluctuate significantly, but hopefully they should always be less than one.

Now you should be ready to take data.

- In the **Data Taking Parameters** pane set **Update Period (Data Run)** to 10s, and **Number of points** to 10. Click the **Take Data** button.

Hopefully you'll find a value of $g^{(2)}(0)$ that is several standard deviations below 1; if you don't, ask for help. Calculate how many standard deviations your value for $g^{(2)}(0)$ is below 1.

- Take several more data sets with different parameters for **Update Period (Data Run)** and **Number of points**. Always take at least 10 points in order to assure reasonable statistics.

Note that while the ideal theoretical prediction for $g^{(2)}(0)$ of a single photon is 0, experimentally you can't achieve this. Try and adjust the experimental parameters so that you get a data set for which the standard deviation of $g^{(2)}(0)$ is several times smaller than the average value of $g^{(2)}(0)$. In other words, try to get a measurement of $g^{(2)}(0)$ which is different from 0 by more than one standard deviation.

- ♦ **Q3: Why can't you measure a value of 0 for $g^{(2)}(0)$?**

- ◆ Q4: When it's done taking data, the computer spits out a value for $g^{(2)}(0)$ that it calls the "expected" value. What is this? Does your measured value for $g^{(2)}(0)$ agree with this expected value (to roughly within the error of the measurement)?

VII. Two-Detector Measurement of $g^{(2)}(0)$

When you've completely finished making measurements on the single photon state, you are ready to show that a single beam of your downconversion source is classical.

- Run the "Coincidence.vi". Set **Experimental Setup** to **$g^{(2)}(0)$ 2-det**, and **Update Period** to 1.0s [this plays the role of T in Eq. (3)]. The computer uses the **BB' Coincidence Window (ns)** parameter as Δt in Eq. (3); ask your instructor what value to use for this parameter (again it should be on the order of 5-10 ns, but won't necessarily be the same as you used for 3-detector measurements). In the pane that displays the graphs, choose the **$g^{(2)}(0)$** tab.
- Adjust the half-wave plate so that the **B** and **B'** counts are about equal.

The $g^{(2)}(0)$ measurements will fluctuate significantly, but hopefully they should always be around one, or greater.

- Click **Clear Buffer** and get an idea of the average value of $g^{(2)}(0)$.

Now you should be ready to take data.

- In the **Data Taking Parameters** pane set **Update Period (Data Run)** to 10s, and **Number of points** to 10. Click the **Take Data** button.

Hopefully you'll find a value of $g^{(2)}(0)$ that is greater than or equal to 1. If you don't, ask for help. Likely you will find that $g^{(2)}(0)$ is equal to 1 within the error of the measurement.

- Take several more data sets with different parameters for **Update Period (Data Run)** and **Number of points**. Always take at least 10 points in order to assure reasonable statistics.

You've just shown that if you condition your measurements on the presence of a photon in the idler beam, you produce a single photon state in the signal beam. This is a highly non-classical state. If you don't condition your measurements, your signal beam behaves classically.

VII. Write-up

Your write-up should include:

- Answers to all questions.
- A table listing your results. For every data run you take I want to see information on parameters you used, and what results you obtained.
- A brief (less than one page) write-up describing what you did in the lab, and summarizing your results. Feel free to comment on the lab as well: what worked, what didn't, and what might be improved.

References:

- [1] P. Grangier, G. Roger, and A. Aspect, "Experimental evidence for a photon anticorrelation effect on a beam splitter: A new light on single-photon interferences," *Europhys. Lett.* **1**, 173-179 (1986).
- [2] J.J. Thorn, M.S. Neel, V.W. Donato, G.S. Bergreen, R.E. Davies, and M. Beck, "Observing the quantum behavior of light in an undergraduate laboratory." *Am. J. Phys* **72**, 1210-1219 (2004).
- [3] G. Greenstein and A. G. Zajonc, *The Quantum Challenge, Modern Research on the Foundations of Quantum Theory*, 2nd ed. (Jones and Bartlett, Sudbury, MA, 2006) Ch. 2.

Appendix A - Coincidence.vi

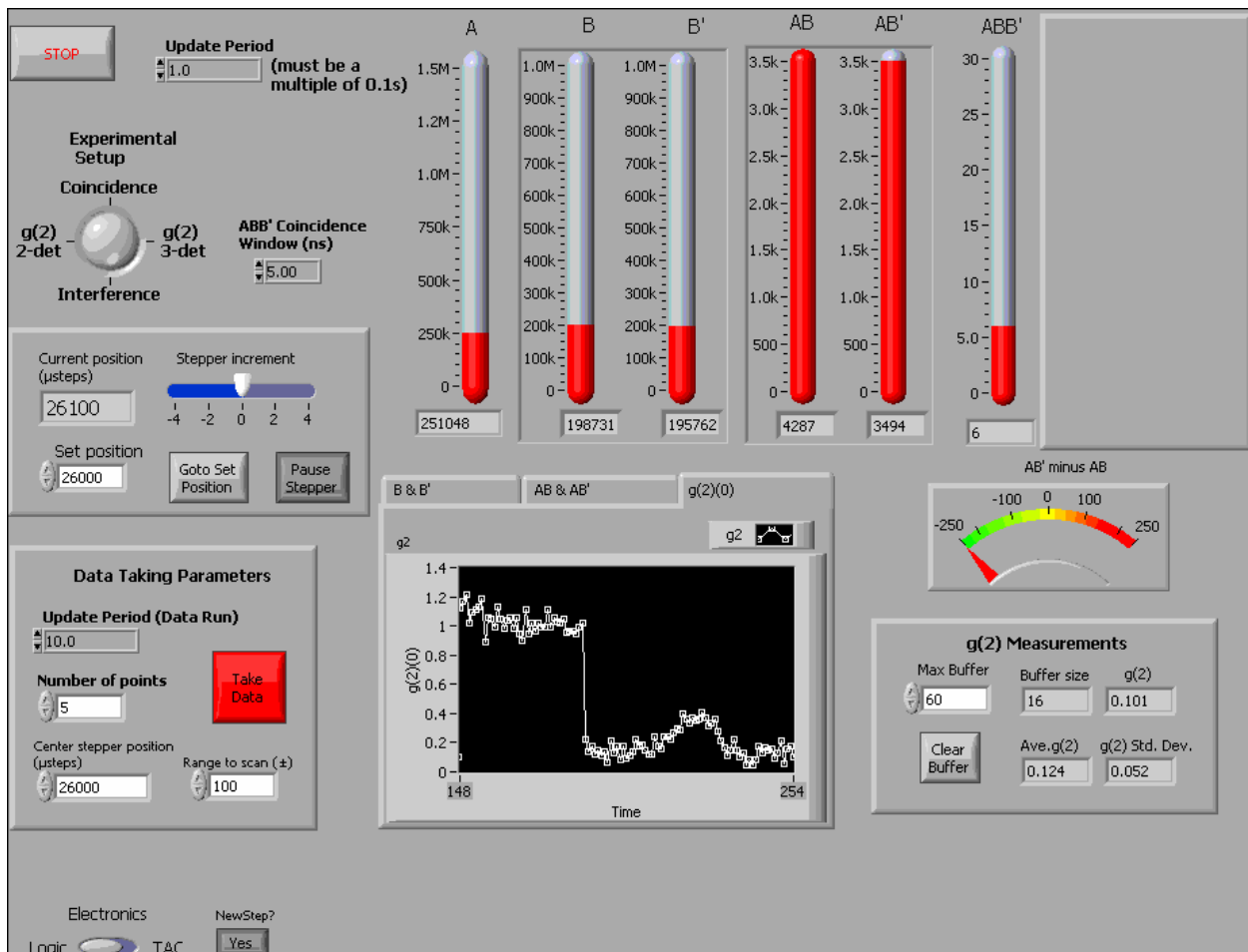
This appendix describes the LabView vi used to acquire data for several experiments: coincidence measurements, proving the existence of photons, and single photon interference.

I. Starting Out

The appearance of this vi will change depending on the experiment you are doing (as determined by the **Experimental Setup** knob on the vi.) The experiment with the most controls and indicators is the interference experiment, and the front panel for this experiment is shown below. If you are doing a different experiment, some of the objects may not be visible.

Coincidence.vi

Front Panel



Description

This is the program you use to run one of 4 different experiments:

- 1) Simply measuring coincidences between two beams.
- 2) Measuring $g(2)(0)$ for 2-beams using 3-detectors.
- 3) Measuring single photon interference patterns.
- 4) Measuring $g(2)(0)$ for 1-beam using 2-detectors.

Note that $g(2)$ is calculated differently depending on whether you're making 3-detector or 2-detector measurements. The calculation also depends on whether you're using the logic circuit (default) or TAC's to do the coincidence detection. See details in the description of the "g(2) Measurements" parameter.

The program does not record data to a file right away, but displays the counters in real time so that you can align things.

Once everything is aligned and the parameters are set, you press the "Take Data" button. This transfers control to another program which records a data set and saves it to a file.

Uses a National Instruments PCI-6602 and reads counters 0 thru 7. The device number for this board should be set to 2. Input to this board is via the Whitman/Trinity coincidence circuit (or via a BNC-2121 connector block for TAC measurements).

Note that there are two controls: "Electronics" and "NewStep?" that tell the computer what hardware you have present in your experiment. These controls are not visible normally. They are located below the "Data Taking Parameters", so you'll need to scroll the window down to access them. These two parameters are only read once at the beginning--so they must be properly set BEFORE you run the program.

The "Electronics" control determines which signals are present on which counters, and also determines how $g(2)$ is calculated (more details below). By default "Electronics" is set to "Logic" for the coincidence circuit.

The "NewStep?" control tells the computer whether or not you have a NewStep stepper motor attached to your computer to control phase adjustments of the interferometer. This control is useful so that the computer won't try to communicate with an instrument you don't have, causing a hang-up. By default "NewStep?" is set to "No"--if you do have a NewStep, you'll want to change the default to "Yes". For more info see the description of this control below.

If using the logic circuit the clock should be set to 10Hz for proper gating of the counters. If you don't use the Whitman/Trinity circuit you will need to have a 0-5V, 10Hz square wave in order to gate the counters. Connect it to the Gate 0 (PFI 38) connector on the PCI-6602 (via the BNC-2121).

For interference measurements, a Newport NewStep actuator (inexpensive stepper motor) is used to tilt a beam displacing polarizer to adjust the phase of a polarization interferometer. This actuator is controlled by a NewStep controller, connected to the serial port of the computer with an RS-485 to RS-232 converter. If you do not have this controller, set the "NewStep?" parameter to "No".

The inputs connect to the sources (SRCn) for the individual counters. This is automatically accomplished with the Whitman/Trinity circuit.

Electrical connections for counters:

When using Logic: (there are automatically made with the Whitman/Trinity circuit)

- A (Counter 0): PFI 39
- B (Counter 1): PFI 35
- B' (Counter 3): PFI 27
- AB (Counter 4): PFI 23
- AB' (Counter 6): PFI 15

ABB' (Counter 5): PFI 19
BB' (Counter 7): PFI 11
Unused A' (Counter 2): PFI 31

When using TACs:

A (Counter 0): PFI 39
B (Counter 1): PFI 35
B' (Counter 3): PFI 27
AB (Counter 4): PFI 23
AB' (Counter 6): PFI 15
ABB' (or just BB' for 2-det measurement) (Counter 5): PFI 19
A Valid Start (from back of AB TAC) (Counter 2): PFI 31
B Valid Start (from back of ABB' TAC) (Counter 7): PFI 11s

Note that for the coincidence experiment, only 3 counters are needed: A, B, and AB. For the other 3 experiments, 7 counters are needed. When making TAC measurements the A & B Valid Start measurements are used to determine the normalization for $g(2)$, not the raw A & B counts.

Note that if you're using the BNC-2121 connector block, the A, B, and B' outputs should be terminated on the block into 50 ohms. The coincidence and Valid Start outputs are terminated straight into the BNC-2121.

On startup, the program initializes the counters.

After initialization the program simply loops and displays the counts in a given time window (determined by the "Update Period" control in the upper left.) This is useful for tweaking the alignment and adjusting parameters.

Nothing is written to disk until the parameters are chosen and the "Take Data" button is pressed. This loads a second VI that records and saves data to disk. Parameters for this data acquisition phase are set in the "Data Taking Parameters" box.

When performing an interference experiment, the stepper motor will automatically adjust the tilt of the beam displacing prism, changing the phase.

Help for each of the controls and indicators can be obtained from the Contextual Help window <ctrl - H> by mousing over each control or indicator. Full documentation for each control and indicator can be obtained by printing using: File>Print>Custom, and then checking "All controls" and "Descriptions".

Controls and Indicators

Coincidence Measurements



Experimental Setup

Which measurement to perform.

Coincidence: Measures A, B, and AB counts.

$g(2)$ 3-det: Make $g(2)$ measurements on 2 correlated beams using 3-detectors. This is

the single photon measurement.

Interference: interference measurement [with simultaneous $g(2)$ 3-detector measurement]

$g(2)$ 2-det: Make $g(2)$ measurements on a single beam using 2-detectors. This is the classical field measurement.



Stop

Use this to stop. If you stop some other way you'll probably need to quit LabView and restart; you may even need to reboot the computer.



Electronics

Which coincidence electronics are being used.

This is important because different electronics have different signals connected to the various counters. It also influences the formulas that are used to calculate $g(2)$.



Update Period

[Must be a multiple of 0.1s]

Time window (in s) for the counters during setup phase (i.e., before the "Take Data" button is pressed.) Readings update once each time window if "Status" reads "Reading Counters".



Counts A, B

Singles counts in the time window specified by "Update Period" (upper left)



Counts AB

Coincidence counts in the time window specified by "Update Period" (upper left)



AB Plot

Chart displaying history of AB coincidence counts



Update Period (Data Run) [Data Taking Parameter]

[Must be a multiple of 0.1s]

Time window (in s) for counters during data acquisition.

This applies after the "Take Data" button has been pressed.



Number of points [Data Taking Parameter]

Number of measurements that are made during data acquisition.

Error measurements are essentially useless if this is less than 5. 10 is a better minimum number. For interference measurements, you will want to use many more than this so you can better see the pattern.



Take Data [Data Taking Parameter]

Leave the setup "tweaking" mode and switch to data acquisition mode.



Func Gen?

Control function generator w/ GPIB?

If No, no GPIB commands are sent. Useful so that the program won't hang if you don't have a GPIB controlled function generator. However, in this case you still need to have a 0-5V, 10Hz square wave input to PFI38 (Gate 0) to use as a clock.

If Yes, the vi uses GPIB to sets the function generator to output a 0-5 V, 10Hz square wave to use as the clock. I still recommend using the SYNC output from the generator-- then only the frequency matters.

This parameter is only read once, when the vi first starts to run. Therefore, it needs to be set BEFORE you run the program.



NewStep?

Is the NewStep controller present?

If No, there is no attempt to communicate with the NewStep controller. Useful if you don't have a NewStep controller. In this case, the "Interference" experiment is unavailable. If you set "Experimental Setup" to "Interference", the program will act as though it's set to "g(2) 3-det".

If Yes, the NewStep functions normally.

This parameter is only read once, when the vi first starts to run. Therefore, it needs to be set BEFORE you run the program.

3-Detector g(2) Measurements

All of the above parameters apply, plus the following:



ABB' Coincidence window

Coincidence window for ABB' measurements.

Used to determine expected g(2) for 3-detector (single-photon) measurements. Basically, this parameter determines the number of expected accidental ABB' counts.



Counts A, B, B'

Singles counts in the time window specified by "Update Period" (upper left)



Counts AB, AB'

Coincidence counts in the time window specified by "Update Period" (upper left)



Counts ABB'

Three-fold coincidence counts in the time window specified by "Update Period" (upper left)



Counts A VS

A Valid starts.

Only used for TAC measurements. Comes from valid start output of AB TAC, and is connected to Counter 2.

This is useful for measuring how many starts get triggered from the A detector. For A rates of about 100k/S or less, the Avs will be slightly less than A (within about 10%). For larger A rates, this can be significantly less than A. Really should keep this rate so that Avs is within 10% of A.



Counts B VS

B Valid starts.

Only used for TAC measurements. Comes from valid start output of ABB' or BB' TAC, and is connected to Counter 7.

On 3-detector g(2) measurements, when measuring three-fold ABB', this is useful for determining whether the start gate is functioning properly. If the start gate delay is set right, then Bvs should be greater than the AB coincidences.

On 2-detector g(2) measurements, when measuring two-fold BB', this is useful for measuring how many starts get triggered from the B detector. For B rates of about 100k/S or less, the Bvs will be slightly less than B (within about 10%). For larger B rates, this can be significantly less than B. Really should keep this rate so that Bvs is within 10% of B.



AB' minus AB

Displays the difference in counts between the AB' and AB counters. Useful for getting the beamsplitter to split 50/50 by balancing the these counts.



g(2) Measurements

The program calculates g(2) for every loop--and this value is displayed as **g(2)**.

Calculated differently depending on which experiment you're doing.

Formulas:

T: update period (counting window, in S)

dt: BB' coincidence window (in nS)

3-detector, 2-beam experiment:

$$g(2)=(A_{vs}^2*ABB')/(A*AB*AB') \quad \text{TAC}$$

$$g(2)=(A*ABB')/(AB*AB') \quad \text{Logic}$$

2-detector, 1-beam experiment:

$$g(2)=(BB'/(B_{vs}*B'))*(T/(dt*1.0e-09)) \quad \text{TAC}$$

$$g(2)=(BB'/(B*B'))*(T/(dt*1.0e-09)) \quad \text{Logic}$$

These g(2) measurements are then stored in an array, which contains the most recent measurements.

g(2) Ave. and **g(2) Std. Dev** are the mean and standard deviation of these stored measurements.

Max Buffer is the maximum size of this array (i.e., the largest number of measurements that will be averaged).

Buffer size is the current length of the array that is being averaged.

Clear Buffer clears out the array, and new measurements begin repopulating it.



Charts

Click on the tabs to display running plots of different measurements: **B & B'**, **AB & AB'**, or **g(2)**.

Interference Measurements

Interference measurements assume a 3-detector setup for g(2) calculations.

All of the above parameters apply, plus the following:



Current position (μ steps)

Current position of the stepper motor.

26000 is about the center of the range with the mount we are using.



Stepper increment

Amount that the stepper increments on each loop if the "Pause Stepper" button is off.



Set position

Force the stepper motor to go to this position by pushing the "Goto Set Position" button.

26000 is about the center of the range with the mount we are using.



Go To Set Position

Forces the stepper motor to go to the "Set position".



Pause stepper

If this is in, the stepper motor is stopped. If it is out, the stepper increments by "Stepper increment" on each loop.



Center stepper position (μ steps) [Data Taking Parameter]

Center of the range for the stepper during data acquisition.



Range to scan (\pm) [Data Taking Parameter]

Range for the stepper during data acquisition.

At each point of data acquisition, the stepper moves evenly between ("Center stepper position" - "Range to scan") and ("Center stepper position" + "Range to scan")

2-Detector $g(2)$ Measurements

All of the above parameters apply, plus the following:



BB' Coincidence window

Coincidence window for BB' measurements.

Needed to determine $g(2)$ for 2-detector (classical) measurements.



2D window stdev

Standard deviation of coincidence window for BB' measurements.

Needed to determine the error in $g(2)$ for 2-detector (classical) measurements.



BB' BB' coincidences.

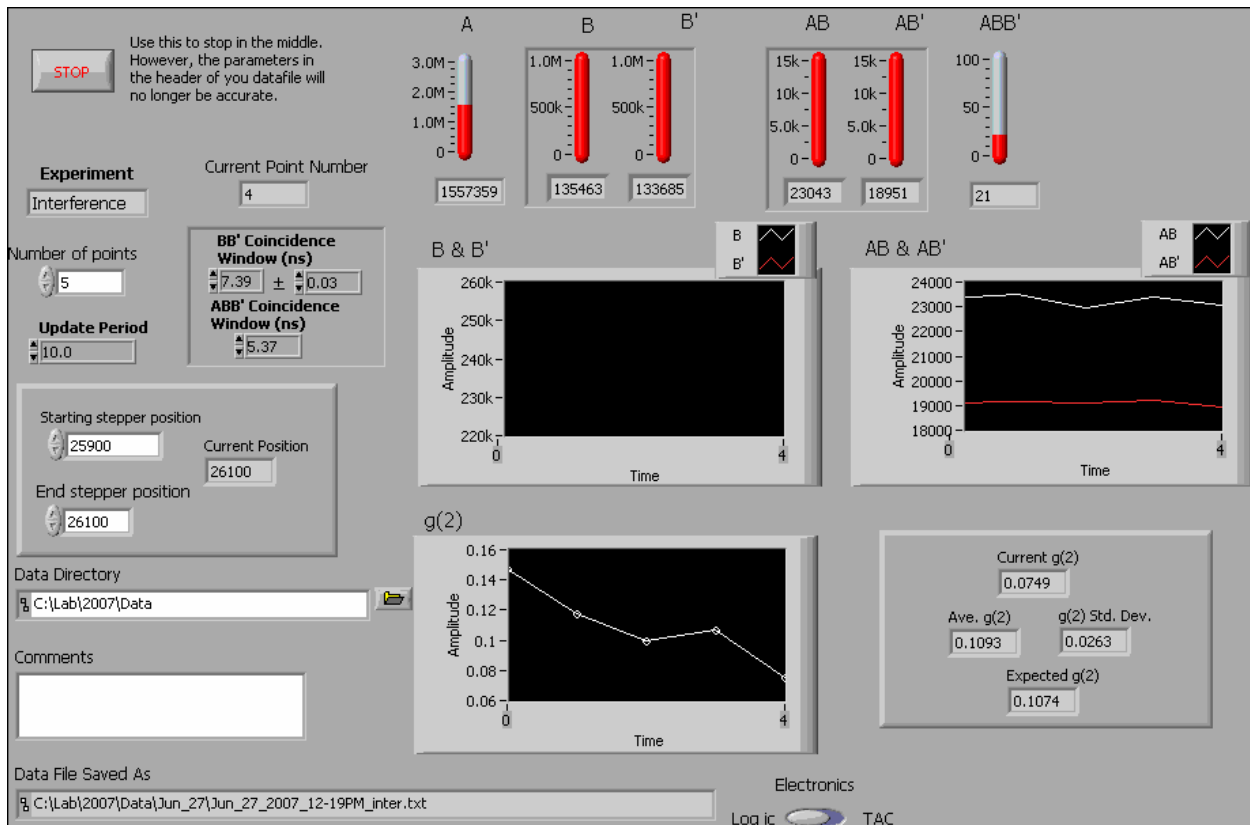
Only used for 2-detector $g(2)$ measurements. Comes from counter 5 for TAC measurements, and counter 7 for Logic measurements.

II. Taking Data

When you move to data taking mode, the program you see will look something like that shown below. Again, the appearance of this vi will change depending on the experiment you are doing.

Coincidence Recorder.vi

Front Panel



Description

This VI should ONLY be called from the "Coincidence" VI--necessary parameters are set there. This program records data (using parameters set in the "Coincidence.vi") and saves the data to a file. For a more detailed description of the parameters, see "Coincidence.vi" .

Controls and Indicators



Stop

Use this to stop in the middle of a data run. However, the parameters in the header of your datafile will no longer be accurate (e.g., you won't have as many points as the header says.)

Also, if you stop some other way you'll probably need to quit LabView and restart; you may even need to reboot the computer.



Experiment

Displays which experiment is being performed: Coincidence, $g(2)$, or Interference.



Number of points

Number of measurements that are made during data acquisition.



Current Point Number

The data point that the computer is currently acquiring.



ABB' Coincidence window

Coincidence window for ABB' measurements.

Used to determine expected $g(2)$ for 3-detector (single-photon) measurements. Basically, this parameter determines the number of expected accidental ABB' counts.



BB' Coincidence window

Coincidence window for BB' measurements.

Needed to determine $g(2)$ for 2-detector (classical) measurements.



BB' 2D window stdev

Standard deviation of coincidence window for BB' measurements.

Needed to determine the error in $g(2)$ for 2-detector (classical) measurements.



Update Period

Time window (in s) for counters during data acquisition.



Data Directory

Path to directory where the data will be saved.



Comments

A space where you can enter comments about the data run. These get saved in the header of the data file.

Once you've entered the text, note that you must hit "Enter" on the NUMERIC KEYPAD, not the "Enter" (or "Return") on the regular keyboard for this text to be saved.



Data File Saved As

Path to the data file. The data file is automatically named using the date and time.



Counts A, B, B'

Singles counts in the time window specified by "Update Period" (upper left)



Counts A VS, B VS

Valid Start counts (only used with TAC)



Counts AB, AB'

Coincidence counts in the time window specified by "Update Period" (upper left)



Counts ABB'

Three-fold coincidence counts in the time window specified by "Update Period" (upper left)



Graphs

Displays graphs of B and AB [Coincidence measurement], or **B & B'**, **AB & AB'**, and **g(2)**. [g(2) and Interference measurement.]



Ave. AB [Coincidence measurement only]

Average value of AB coincidences. Updated when program ends.



AB Std. Dev. [Coincidence measurement only]

Standard deviation of AB coincidences. Updated when program ends.

g(2) Measurements (both 2-Detector and 3-Detector)

All of the above parameters apply (except "Ave. AB" and "AB Std. Dev."), plus the following:



Current g(2)

g(2) measurement for the current data point.



Ave. g(2)

Average of the g(2) measurements.



g(2) Std. Dev.

For 3-detector measurements this is the standard Deviation of the g(2) measurements.

For 2-detector measurements during data acquisition it is the standard deviation of the g(2) measurements. At the end this error is added in quadrature with the error in g(2) due to the uncertainty of the BB' coincidence time window ("BB' 2D window stdev").



Expected g(2)

Calculate the expected value of the parameter g⁽²⁾ (0). Based on number of expected accidental coincidences.

Calculated differently depending on which experiment you're doing, and which electronics you're using.

For 2-detector, 1-beam measurements, this is assumed to be 1.0 (a classical beam).

For all other measurements, when the vi first starts running it is set to 0.0, and is updated with the expected g(2) at the very end.

Formula (from Appendix A of Thorn AJP)

T: update period (counting window, in S)

dt: ABB' coincidence window (in nS)

$$g(2) = (dt * 1.0e-09 / T) * A_{vs} * ((B/AB) + (B'/AB')) \quad \text{TAC}$$

$$g(2) = (dt * 1.0e-09 / T) * A * ((B/AB) + (B'/AB')) \quad \text{Logic}$$

Interference Measurements

Interference measurements assume a 3-detector setup for g(2) calculations.

All of the above parameters apply (except "Ave. AB" and "AB Std. Dev."), plus the following:



Starting stepper position

Position of stepper motor at start of scan.



End stepper position

Position of stepper motor at end of scan.

Over the course of a data run, the motor steps evenly between the starting and ending positions.



Current Position

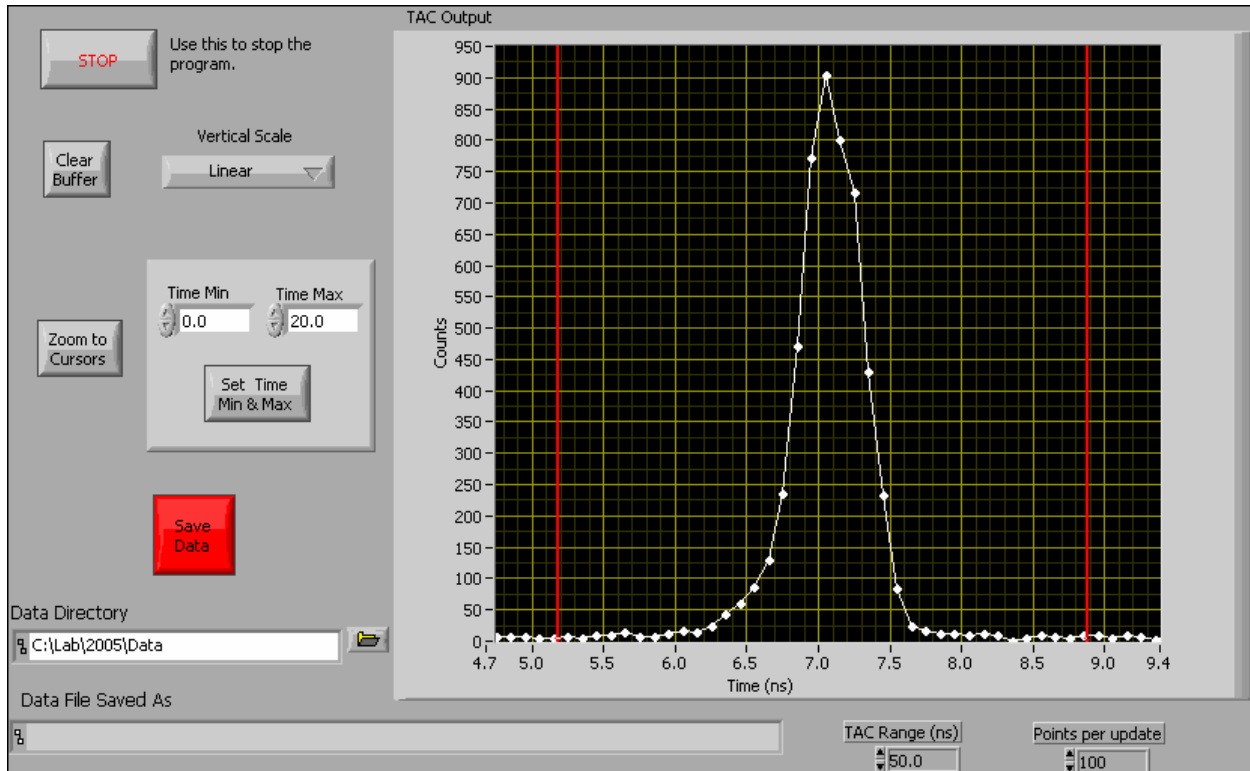
Position of stepper motor for the current data point.

Appendix C - MCA.vi

This appendix describes the LabView vi used to mimic the behavior of a multichannel analyzer (MCA). This is useful for measuring the arrival time of photons.

MCA.vi

Front Panel



Description

This VI emulates a multi-channel-analyzer (MCA). An MCA essentially digitizes a series of voltage pulses, and creates a histogram of the pulse heights. The purpose of this VI is to analyze at the voltage pulses from a Time-to-Amplitude Converter (TAC) [This VI was tested using the TAC in an ORTEC 567 TAC/SCA module].

The start and stop pulses going into the TAC come from photon counters, and the TAC output voltage is proportional to the time between the start and stop. Thus, the MCA is creating a histogram of the time interval between the arrivals of the two photons.

The main difference between this VI and a real MCA is that an MCA takes only one input—the voltage pulses. This VI also needs timing information about when the pulses are arriving. Fortunately, this can be obtained from the Valid Conversion output of the TAC. The Valid Conversion output is an approximately 3 microsecond long TTL pulse coincident with the TAC output pulse.

We have tested this VI with 2 different National Instruments A/D cards: 6036E and 6052E. With these cards there are two clock signals that are needed to perform an A/D conversion: the Scan Clock and the Channel Clock.

The Scan Clock (input through PFI0) comes directly from the Valid Conversion output of the TAC. The program is configured to initialize a scan on a low-to-high transition of the Scan Clock (edit the program if you want a high-to-low transition) -initializing a scan arms the A/D, but does not actually cause an A/D conversion.

The Channel Clock (input through PFI2) follows the Scan Clock, and a the program is configured to perform an A/D conversion on a high-to-low transition of the Channel Clock (edit the program if you want a low-to-high transition). The Channel Clock is obtained from the output of an HP33120A waveform generator. The 33120A is externally triggered by the Valid Convert output of the TAC, and on each trigger it outputs a 0.5 microsecond pulse. The 33120A is operated in burst mode to accomplish this-the VI programs the 33120A with the correct parameters when it first starts. The 33120A is programmed over GPIB, and must be at GPIB address 9.

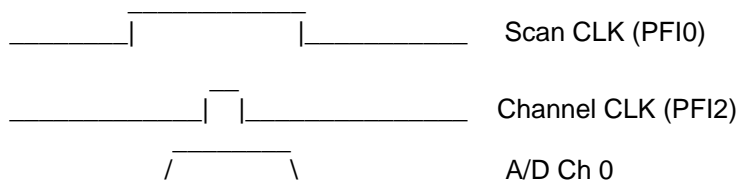
The TAC output to be digitized is input though Analog Input Channel 0.

Unlike many VI's you'll encounter, the screen updates after a specified number of data points are acquired (determined by the parameter "Points per update"), not after a specific time interval. Because of this, if the detectors are off, nothing will happen.

NOTE: The A/D boards we use are just barely fast enough to catch the 3 microsecond long TAC output--indeed, they're probably technically too slow. Because of this, the accuracy of the measurement of the TAC output is not very good (can be off by as much as 10 or 20%), which means that the time scale is poorly calibrated. However, the measurement is repeatable, so the time scale could be calibrated much more accurately. Despite this problem, the VI works quite well enough to accomplish its main goals-to display a bump in the histogram of arrival times between the photons from two detectors, and to allow one to set the SCA window to select coincidences.

ALSO NOTE: This vi has only been seriously tested for START-STOP times ranging from a few up to about 30 ns. With much longer intervals than this the output pulses may be delayed, and the timing may change.

Rough Timing diagram:



Help for each of the controls and indicators can be obtained from the Contextual Help window <ctrl - H> by mousing over each control or indicator. Full documentation for each control and indicator can be obtained by printing using: File>Print>Custom, and then checking "All controls" and "Descriptions"

Controls and Indicators

 **Stop**
Use this to stop.

 **Clear Buffer**

Clears the histogram memory, and the accumulation starts over again.



Vertical Scale

Change the scaling of the vertical scale. Options are Linear and Logarithmic.



Zoom to cursors

Horizontal scale will zoom in to the region specified by the cursor positions.



Time Min

Set minimum of horizontal axis to this value after pressing "Set Time Min & Max".



Time Max

Set maximum of horizontal axis to this value after pressing "Set Time Min & Max".



Set min & max

Set the minimum and maximum values of the horizontal axis to those specified.



Save Data

Save the current data to a file. Program exits after this is done.



Data Directory

Path to directory where the data will be saved.



Data File Saved As

Path to the data file. The data file is automatically named using the date and time.



TAC Range (ns)

The full scale range of the TAC output. Used to scale the horizontal axis.



Points per update

Number of data points acquired before updating the screen. Remember, the screen updates after a specified number of data points are acquired, not after a specific time interval.

If you have very low count rates, you might want to decrease this from its default value of 100.



TAC Output

Histogram of the time interval distribution.

